Int J Earth Sci (Geol Rundsch) (2003) 92:743–757
DOI 10.1007/s00531-003-0343-x

ORIGINAL PAPER

Kai Kessels · Jörg Mutterlose · Alastair Ruffell

Calcareous nannofossils from late Jurassic sediments of the Volga Basin (Russian Platform): evidence for productivity-controlled black shale deposition

Received: 4 June 2002 / Accepted: 24 May 2003 / Published online: 11 September 2003

Abstract The Jurassic/Cretaceous boundary interval in the northern hemisphere is characterized by the widespread occurrence of black shales. About 60% of all petroleum source rocks comprise sediments of late Jurassic and early Cretaceous age with the origin of such black shales still under discussion. In order to better understand the factors that controlled black shale sedimentation, 78 samples were analyzed for calcareous nannofossils from two sections (Gorodische, Kashpir) of the Volga Basin (NE Russia). Calcareous nannofossils are ideal proxies for deciphering nutrient, temperature and salinity fluctuations. Additionally 58 samples from both sections were also analyzed for clay mineralogy, $\delta^{13}C_{org}$, TOC and $CaCO_3$ composition. Both sections contain calcareous claystones and intercalated organic rich shales overlain by phosphorite beds. The presence of the calcareous nannofossil species *Stephanolithion atmetros* throughout both successions allows a biostratigraphic assignment to the *S. atmetros* Nannofossil Biozone (NJ 17), which corresponds to the *Dorsoplanites panderi* Ammonite Biozone of the Middle Volgian. The marlstones of the Kashpir section yield a well-preserved rich and diverse nannoflora, whereas all black shale beds are essentially barren of calcareous nannofossils. Only the uppermost black shale layers yield an impoverished assemblage of low diversity and abundance. Geochemical data suggest an early diagenetic nannofossil dissolution in the black shales of the Kashpir section. This is supported by the occurrence of coccoliths in black shale horizons of the Gorodische section. The assemblages in both sections are dominated by coccoliths of the Watznaueriaceae group (*Watznaueria barnesae, Watznaueria fossacincta, Watznaueria britannica, Watznaueria communis*), *Biscutum constans* and *Zeugrhabdotus erectus.* In Kashpir rare specimens of *Crucibiscutum salebrosum* occur in the higher part of the section. These taxa indicate boreal affinities. *B. constans* and *Z. erectus* are considered to be taxa indicative of a higher productive environment, while *C. salebrosum* is a cool-water species. From base to top of the Kashpir section, consecutive mass occurrences of different taxa/groups were observed: *W. barnesae–W. fossacincta* acme, *W. britannica–W. communis* acme, *Z. erectus* acme, *B. constans* acme (including sparse occurrences of *C. salebrosum*).

The observed distribution patterns have been interpreted as characterizing a transition from a low productive, oligotrophic setting with high abundances of K-selected cosmopolitan species (Watznaueriaceae) and predominating marlstone sedimentation to a higher productive, mesotrophic setting. Cooler water temperatures marked by r-selection and acmes of opportunistic species (*Z. erectus, B. constans*) are coincident with the deposition of black shales and phosphorites in the higher part of the section. Interpretation of clay mineral distribution indicates that black shale deposition occurred under semi-arid hinterland climatic conditions concomitant with a sea level rise. This induced dysoxic conditions in the deeper parts of the Volga Basin, favoring the preservation of organic matter. The cause of the nutrient enrichment in the surface water is still unclear, but possible river water input from the continents does not seem to have been the controlling factor under a semi-arid climate. The occurrence of phosphorites in the upper part of both sections presumably indicates that enhanced productivity may be better explained by the upwelling of nutrient-rich bottom water and thereby causing the recycling of nutrients from oxidized phytoplankton back into the photic zone. This recycling effect finally may have led to an intensified phytoplankton growth which seemed to be a sufficient source for the enrichment of organic matter. This is well

K. Kessels (✉) · J. Mutterlose
Institut für Geologie, Mineralogie und Geophysik,
Ruhr-Universität Bochum,
44801 Bochum, Germany
e-mail: kai.kessels@ruhr-uni-bochum.de

A. Ruffell
School of Geography,
The Queen's University,
Belfast, BTZ INN, UK

correlated with the increase in black shale horizons in the upper part of the Kashpir section.

Keywords Calcareous nannofossils · Late Jurassic · Black shales · Volga Basin · Paleoproductivity

Introduction

Black shales are sediments rich in organic matter (>1%) and reflect specific environmental conditions such as anoxic–suboxic conditions of bottom waters (Wignall 1994). Black shales have a widespread occurrence throughout the Phanerozoic. In particular, the ocean-wide black shales (OAEs) of the late Jurassic and early Cretaceous have been the target of research over the past 25 years due to their specific setting. Beyond the North Sea and NW Europe, less attention has been paid to late Jurassic black shales, which are common in particular in the northern hemisphere. They have been reported from the North Sea (Kimmeridge Clay) and Siberia. In mid Volgian times (late Jurassic) black shales were extensively deposited in the Volga Basin of the Russian Platform. These "Kashpir" oil shales are presently one of the most important oil shale sources of Russia. Recently only few works studied the diagenesis and formation of these oil shales (e.g., Shmur et al. 1983; Kuleva et al. 1996; Riboulleau et al. 2000).

The paleobiogeography of calcareous nannofossils can be used for the reconstruction of past depositional environments in Mesozoic and Cenozoic oceans. Various studies during the last decades have deciphered important aspects of their paleoecological, oceanographic and climatic significance (e.g., Roth and Bowdler 1981; Roth and Krumbach 1986; Roth 1986, 1989; Premoli-Silva et al. 1989; Watkins 1989; Coccioni et al. 1992; Erba et al. 1992; Eshet and Almogi-Labin 1996; Fisher 1999; Mutterlose and Kessels 2000, Street and Bown 2000; Bersezio et al. 2002; Pittet and Mattioli 2002; Lees 2003). Variations in the composition and abundance of calcareous nannofossils are used as paleoproxies for autecological changes especially of surface water nutrients, detrital input from adjacent landmasses, oceanic currents, water temperatures and salinities. During the Jurassic/Cretaceous boundary interval significant differences in the assemblage composition have been recognized between the Boreal Realm, the Tethyan Realm and the Indo-Pacific area (e.g., Perch-Nielsen 1985; Mutterlose and Kessels 2000; Street and Bown 2000).

The main goals of our work address the following questions:

1. Was the black shale deposition connected to changes in the calcareous nannofossil community?
2. What caused black shale deposition in the late Jurassic Volga Basin?

Geological framework

The Russian Platform Basin

The structural basement of southwestern Russia is formed by the Russian Platform, a cratonic block bounded to the north and west by the Baltic and Ukrainian Shield, to the south by the Caucasus and the Peri-Caspian region and to the east by the Urals (Nalivkin 1973). Vertical tectonic movements and episodes of global sea-level change during most of the Palaeozoic and Mesozoic led to marine transgressions and regressions and therefore the periodic development of a shallow epicontinental sea, the Russian Platform Basin. Due to different subsidence rates its extension varied through the Mesozoic. Sea-ways between the Tethys and the Arctic Sea existed occasionally (Baraboshkin 1999). In Volgian time the width of the basin was about 500 km in an east–west direction and more than 200 km north–south with water depths of 80–150 m (Fig. 1a). Sasonova (1977) considers the Russian Platform Basin to have been located at a palaeolatitude of ~40–50°N in the late Jurassic. A narrow seaway did exist

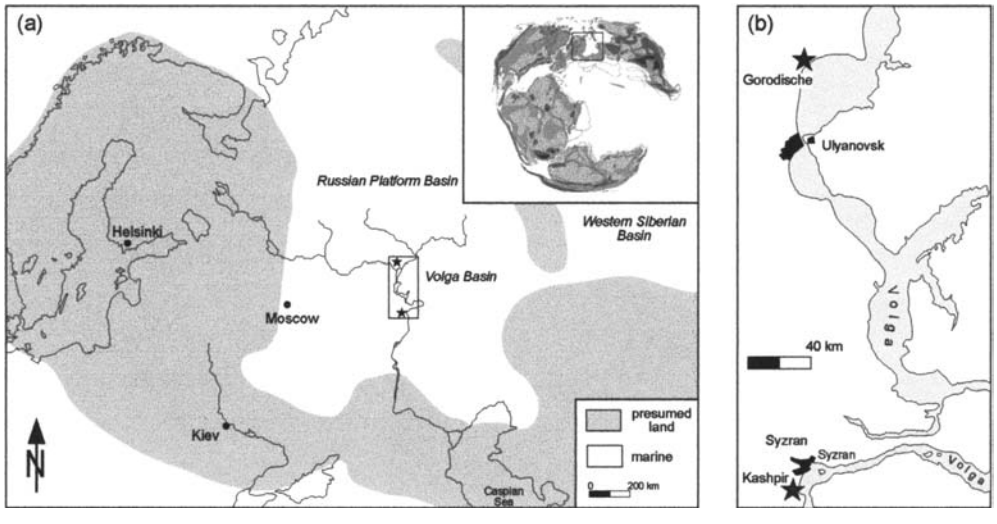

Fig. 1 **a** Paleogeographic map of the Russian Platform in Volgian times (modified according to Sazonov and Sazonova 1967; Baraboshkin 1999); Paleogeographic world map in Volgian times (modified according to "The Paleogeographic Atlas Project," University of Chicago). **b** Geographic overview of the examined sections

to the Western Siberian Basin (Baraboshkin 1999). The localities under consideration are situated in the central part of the Russian Platform Basin, which is also referred to as the Volga Basin (Fig. 1a).

The Kashpir section

Kashpir is situated about 100 km south of Ulyanovsk in the eastern part of the Samara province (Fig. 1b). The studied section (close to Kashpir village on the western bank of the Volga River) is composed of rhythmically bedded calcareous mudstones with intercalated black shale horizons of 0.1 to 0.5 m thickness. These sediments are overlain by cross-bedded silty-sand horizons containing reworked phosphatized fossils and abundant phosphatic nodules. The black shales are dark brown to black, bioturbated (e.g., *Chondrites*) and show no lamination. A detailed description is given by Sasonov and Sasonova (1967) and Gerasimov and Mikhailov (1966). Biostratigraphically, the sampled part is assigned to the mid Volgian *Dorsoplanites panderi* Ammonite Zone and to the NJ17b (*Ethmorabdus gallicus*) boreal Nannofossil Subzone, respectively. The overlaying silt- and sandstones are of late Volgian age (*Kachpurites fulgens—Craspedites nodiger* ammonite zones, Fig. 2). The succession yields a rich macrofauna (e.g., ammonites, belemnites; Gerasimov and Mikhailov 1966).

The Gorodische section

Gorodische is located in the Ulyanovskaya province about 25 km south of Ulyanovsk (Fig. 1b). The studied section is situated close to Gorodische village directly on the western bank of the Volga River and represents the lectostratotype of the Volgian (Gerasimov and Mikhailov 1966). A detailed description of the outcropping sediments is given by Mesezhnikov (1977). The investigated succession comprises middle Volgian, calcareous mudstones alternating with several 0.5- to 1-m-thick black shale horizons and is stratigraphically assigned to the *D. panderi* Ammonite Zone and to the NJ17 (*Stephanolithion atmetos*) Boreal Nannofossil zone, respectively (Fig. 2). The sampled section includes the upper part of the NJ17a (*Axopodorhabdus cylindratus*) Subzone and the lower part of the NJ17b (*Ethmorabdus gallicus*) Subzone. The mid Volgian sediments are overlain by a late Volgian (*K. fulgens–C. nodiger* Ammonite Zones) silty–sandy horizon with phosphatic nodules. The black shales are lithologically similar to those of the Kashpir section—dark brown to black, bioturbated (e.g., *Chondrites*)—and show no lamination. Both the mudstones and the black shales contain abundant macrofossils (e.g., ammonites, belemnites, bivalves, gastropods; Kuleva et al.1996; Hantzpergue et al. 1998a, b).

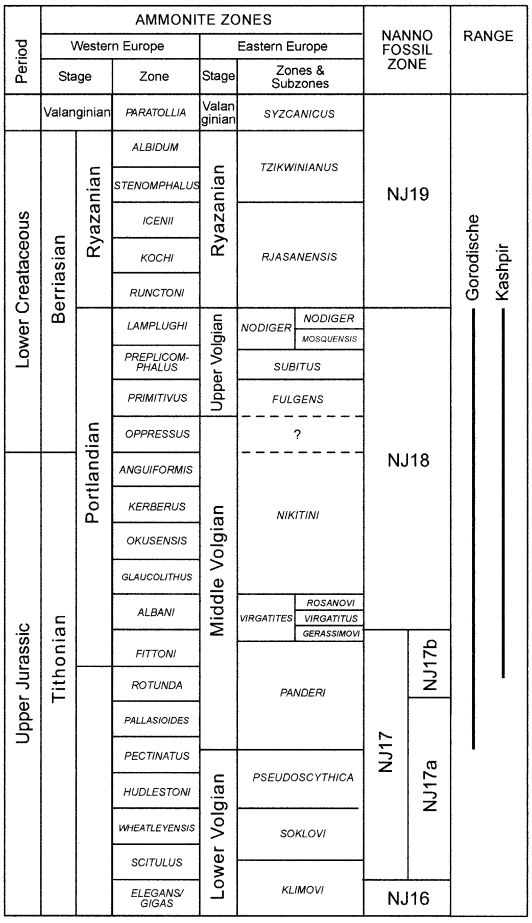

Fig. 2 Stratigraphic range of the Gorodische and Kashpir sections

Material and methods

A total of 78 samples were analyzed from the Gorodische and Kashpir sections with respect to its calcareous nannofossil content. At Kashpir 58, samples from a 5.5-m-thick sequence were studied to document high resolution floral changes. At Gorodische, 20 samples of a 10-m-thick succession have been investigated. Simple smear slides were examined under a Olympus BH-2 light microscope using a magnification of 1500x. To determine the relative abundances of each sample at least 300 specimen or 200 fields of view were counted. Additionally, one traverse of each slide was examined to record rare species.

Species richness (S), heterogeneity (H) and equitability (E) were calculated. Species richness is the number of species in a sample. It depends on the number of counted fields and the specimen density of the slide. Heterogeneity considers both the number of species and their relative abundances. This analytical method highlights the dominance of different species. Equitability is derived from heterogeneity and reveals how evenly the species are distributed among all individuals of a sample. Low values for both heterogeneity and equitability, caused by the dominance of only a few species in an assemblage,

indicate unstable mesotrophic conditions (e.g., Watkins 1989; Dodd and Stanton 1990), following r-selection.

To estimate the state of preservation the following abbreviations have been used: G (very good preservation, no etching), E1 (slightly etched), E2 (moderately etched), E3 (heavily etched), E4 (no coccoliths preserved), O1 (overgrown). Bibliographic references for the encountered taxa are given by Bown (1998), Cooper (1987) and Perch-Nielsen (1985). Nannofossil preparations are placed at the Department of Geology, Mineralogy and Geophysics of the Ruhr-University Bochum.

For the analysis of clay mineralogy 42 fine-grained samples obtained from sample splits of the calcareous nannofossil samples from the Kashpir section were prepared for X-ray diffraction. Both bulk rock and clay fraction analysis were made (according to Tucker 1988). Sample and analytical methodology is described in Ruffell et al. (2002a). The results presented here are largely from the clay fraction analysis.

Carbonate measurements were made using atomic adsorption spectrometry (AAS), organic carbon content was determined by coulometry and $\delta^{13}C_{org}$ was measured at the Geological Institute of the University of Bremen using a Finnigan DELTA-E mass spectrometer. The reproducibility of replicate samples was better than 0.1‰.

Results

Calcareous nannofossils

The most common taxa that were observed are displayed in Figs. 3 and 4.

Preservation—observations

The preservation of calcareous nannofossils shows a wide distribution from very good (G) to totally dissolved (E4). In the Kashpir section a correlation between lithology and preservation was clearly observed. Whereas calcareous mudstones contain generally well-preserved to slightly etched nannofossils, the black shales are essentially barren of coccoliths and only some heavily-etched specimens of robust *Watznaueria* spp. were recognized in the upper part. Nannofossils from the Gorodische section are moderately preserved and exhibit in a few samples evidence for overgrowth. In the Gorodische section (in contrast to Kashpir) calcareous nannofossils have been observed in the black shale-derived samples.

Diversity—observations

Species richness of calcareous nannofossils with a total of 31 identified taxa in both sections is moderate, but no sample contained more than 17 species. The variation of species richness, in Kashpir from 8–16 and in Gorodische from 5–17, is clearly related to different preservation modes and is not ecologically controlled. In general a positive correlation between CaCO3 content and species richness has been observed. Samples of low carbonate content are associated with badly preserved nannofossil assemblages of lower diversity, as it was recognized in nearly all of the black shales horizons of the Kashpir section. Heterogeneity ranges in Kashpir between 0.7 and 2.2 and shows a sharp decrease in the uppermost part of the succession. In Gorodische, heterogeneity is more uniform (1.2 to 2.0) and correlates to the preservation mode of the encountered coccoliths. Equitability ranges in Kashpir from 0.3–0.9, and in Gorodische from 0.5–0.9.

Assemblage composition–observations

The nannofossil assemblages are dominated by only a few species, which are all of paleoecological relevance. They make up more than 90% of all taxa and will be discussed here. These taxa include *Watznaueria* spp., *Biscutum constans*, *Zeugrhabdotus erectus*, *Crucibiscutum salebrosum*, *Cretarhabdus* spp. and *Staurolithites* spp. (Figs. 5, 6)

Watznaueria spp. (*W. barnesae*, *W. fossacincta, W. britannica*, *W. communis*, *W. ovata*) is the most abundant group in all samples investigated. In the lower part of Kashpir this group makes up more than 75% of the total assemblages and clearly decreases down to 25% in the uppermost part of the section. *W. barnesae*, *W. fossacincta, W. britannica* and *W. communis* show similar abundances in both sections. Generally *W. barnesae* and *W. fossacincta* are most common (up to 74%), while *W. britannica* and *W. communis* are less common (up to 43%), *W. ovata* is usually rare with highest abundances of 4% in only a few samples.

B. constans is the second most common species in the Kashpir section. It ranges from 1% in the lowermost part and increases steadily, up to 58%, with the first occurrence of the black shales at the top of the succession. In Gorodische, the distribution of *B. constans* maintains a stable average of 11% over the studied interval. For this taxon, a generally positive correlation with the occurrence of black shales has been observed.

Fluctuations in abundances of *Z. erectus* are very similar to those of *B. constans*. Higher values were only observed in the black shale bearing parts of both section. In these intervals *Z. erectus* makes up to 33% of the total assemblages.

C. salebrosum is clearly restricted to the uppermost part of the Kashpir section. This taxon is, however, rare with highest abundances of 3%. The occurrence of *C. salebrosum* coincides with the highest abundances of *B. constans*. *Cretarhabdus* spp. and *Staurolithites* spp. are quite rare in both sections. These two genera never exceed more than 5% of the total abundances.

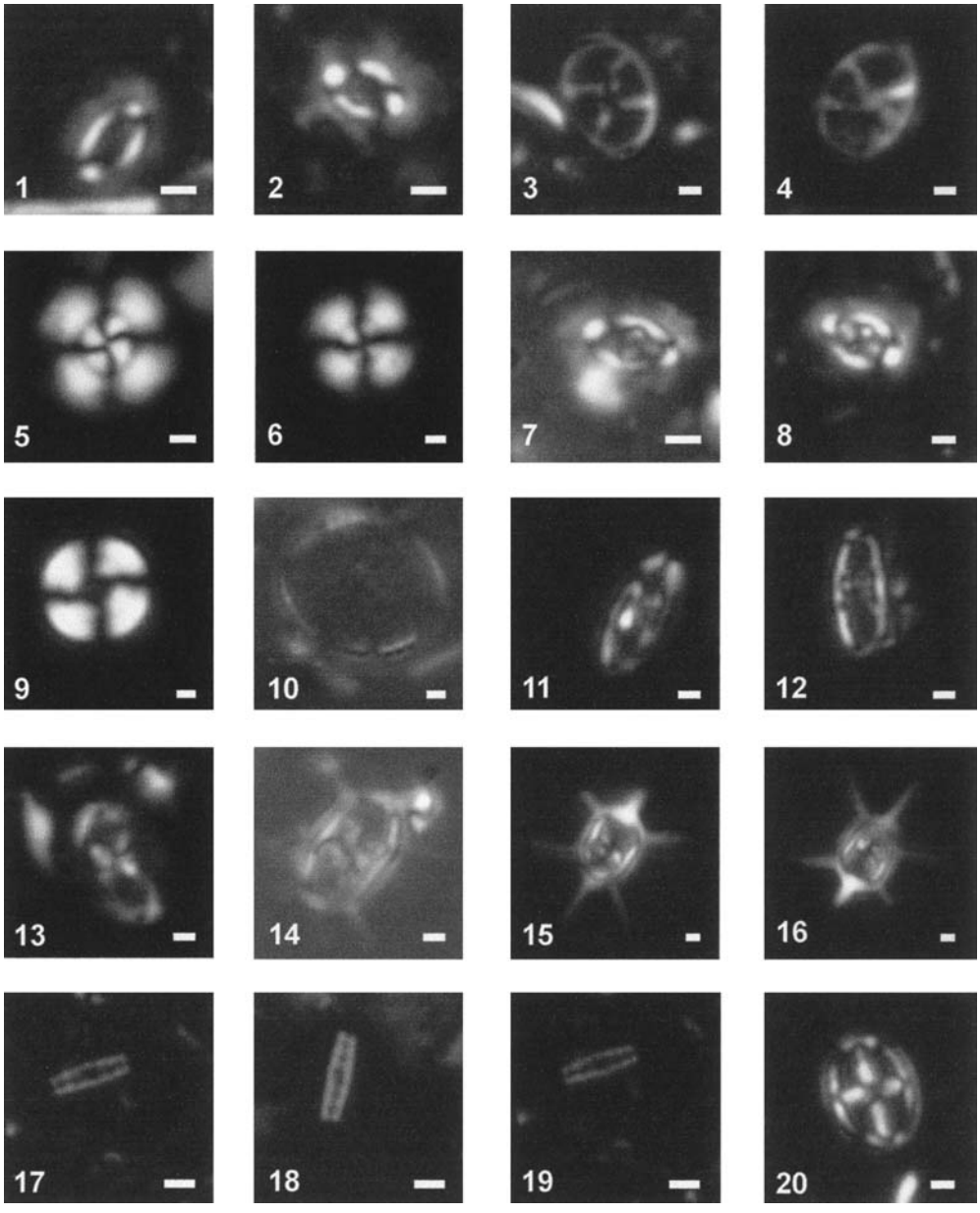

Fig. 3 Calcareous nannofossils. Some of the most common taxa observed: (1)*Biscutum constans* (Górka 1957) Black in Black & Barnes 1959, Sample: Kashpir 97/3 XPL; (2) *Biscutum constans* (Górka 1957) Black in Black & Barnes 1959, sample: Kashpir 97/4 XPL; (3) *Chiastozygus leptostaurus* Cooper 1987, sample: Kashpir 97/4 XPL; (4) *Chiastozygus leptostaurus,* Cooper 1987, sample: Kashpir 93/2; XPL; (5) *Cyclagelosphaera margerelii* Noël 1965, sample: Kashpir 93/2 XPL; (6) *Cyclagelosphaera margerelii* Noël 1965, sample: Kashpir 89/3 XPL; (7) *Crucibiscutum salebrosum* (Black 1971) Jakubowsky 1986, Sample: Kashpir 97/3 XPL; (8) *Crucibiscutum salebrosum* (Black 1971) Jakubowsky 1986, sample: Kashpir 97/3 XPL; (9) *Cyclagelosphaera tubulata* (Grün & Zweili 1980) Cooper 1987, sample: Kashpir 95/1 XPL; (10) *Etmorhabdus gallicus* Noël 1965, sample: Gorodische 88/1 XPL; (11) *Stephanolithion atmetos* Cooper 1987, sample: Kashpir 95/10 XPL; (12) *Stephanolithion atmetos* Cooper 1987, sample: Kashpir 95/10 XPL; (13) *Stephanolithion atmetos* Cooper 1987, sample: Kashpir 95/10 XPL; (14) *Stephanolithion bigotii* Deflandre 1939, sample: Gorodische 88/1 XPL; (15) *Stephanolithion bigotii* Deflandre 1939, sample: Gorodische 88/1 XPL; (16) *Stephanolithion bigotii* Deflandre 1939, sample: Gorodische 88/1 XPL; (17) *Truncatoscaphus intermedius* Perch-Nielsen 1986, sample: Kashpir 97/7 XPL; (18) *Truncatoscaphus intermedius* Perch-Nielsen 1986, sample: Kashpir 91/4 XPL; (19) *Truncatoscaphus intermedius* Perch-Nielsen 1986, Sample: Kashpir 91/4 XPL; (20) *Staurolithites lumina* Bown 1998, sample: Gorodische 90/1 XPL; *white ba* =1 μm

Variation in $\delta^{13}C_{org}$, TOC and $CaCO_3$—observations

The samples of the Kashpir section were prepared to measure their $\delta^{13}C_{org}$, TOC and $CaCO_3$ content. All results are summarized in Fig. 6. $\delta^{13}C_{org}$ values are expressed as the relative differences in isotopic ratios ($^{12}C/^{13}C$) between a sample and the Vienna-PDB standard (δ notation).

The $\delta^{13}C_{org}$ composition ranges from −25 to −22‰. Two general trends have been observed: first, a slight

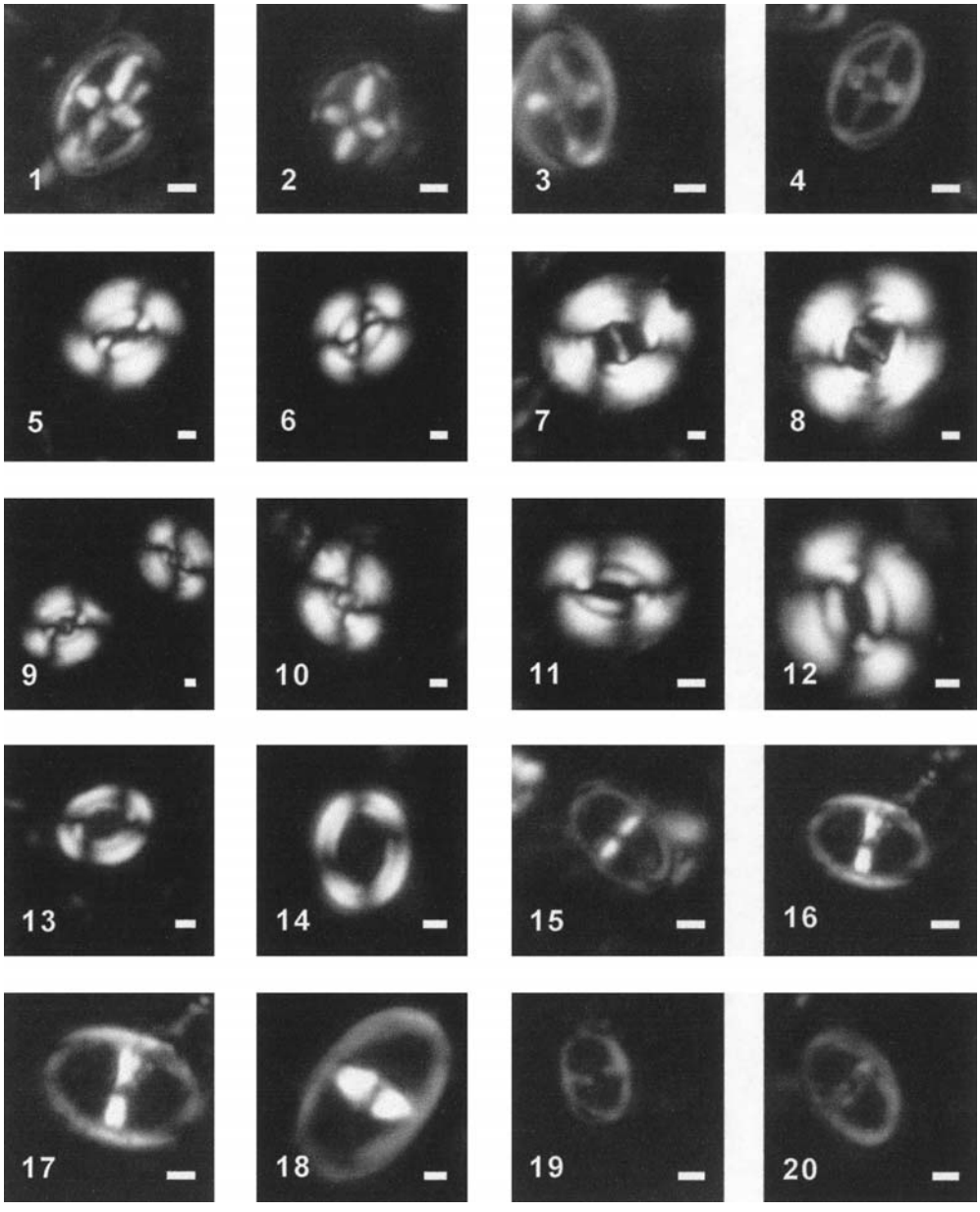

Fig. 4 Calcareous nannofossils. The rest of the most common taxa observed: (1) *Staurolithites lumina* Bown 1998, sample: Gorodische 90/1 XPL; (2) *Staurolithites lumina* Bown 1998, sample: Gorodische 90/1 XPL; (3) *Staurolithities stradneri* Rood et al. 1971, sample: Kashpir 95/3 XPL; (4) *Staurolithites quadriaculla* (Noël 1965) Rood et al. 1971, sample: Kashpir 95/3 XPL; (5) *Watznaueria barnesae* (Black 1959) Perch-Nielsen 1968, sample: Gorodische 86/1 XPL; (6) *Watznaueria barnesae* (Black 1959) Perch-Nielsen 1968, sample: Kashpir 87/4 XPL; (7) *Watznaueria britannica* (Stradner 1963) Reinhardt 1964, sample: Kashpir 97/3 XPL; (8) *Watznaueria britannica* (Stradner 1963) Reinhardt 1964, sample: Kashpir 97/3 XPL; (9) *Watznaueria communis* (Stradner 1963) Reinhardt 1964, sample: Kashpir 95/4 XPL; (10) *Watznaueria communis* (Stradner 1963) Reinhardt 1964, sample: Gorodische 88/1 XPL; (11) *Watznaueria fossacincta* (Black 1971) Bown in Bown & Cooper 1989, sample: Kashpir 91/4 XPL; (12) *Watznaueria fossacincta* (Black 1971) Bown in Bown & Cooper 1989, sample: Kashpir 95/1 XPL; (13) *Watznaueria ovata* Bukry 1969, sample: Kashpir 91/4 XPL; (14) *Watznaueria ovata* Bukry 1969, sample: Kashpir 91/4 XPL; (15) *Zeugrhabdotus erectus* (Deflandre in Deflandre & Fert 1954) Reinhardt 1965, sample: Kashpir 97/7 XPL; (16) *Zeugrhabdotus erectus* (Deflandre in Deflandre & Fert 1954) Reinhardt 1965, sample: Kashpir 97/7 XPL; (17) *Zeugrhabdotus erectus* (Deflandre in Deflandre & Fert 1954) Reinhardt 1965, sample: Kashpir 97/7 XPL; (18) *Zeugrhabdotus erectus* (Deflandre in Deflandre & Fert 1954) Reinhardt 1965, sample: Kashpir 91/4 XPL; (19) *Zeugrhabdotus erectus* (Deflandre in Deflandre & Fert 1954) Reinhardt 1965, sample: Kashpir 91/4 XPL; (20) *Z. fissus* Grün & Zweili 1980, sample: Gorodische 91/1 XPL; white bar=1μm

increase of $\delta^{13}C_{org}$ from the base to the top was recognized and secondly, all black shale horizons are characterized by positive excursions of $\delta^{13}C_{org}$ with maximum values of −22‰. Total organic carbon is clearly correlated to lithology and varies between 0.2 and 11.8%. Higher values were measured in nearly all of the black shale layers, whereas the marly samples contain a maximum 1% of TOC. In contrast, CaCO3 contents are notably higher in

Fig. 5 Relative abundances (counts) of calcareous nannofossils of **a** Gorodische and **b** Kashpir section. *Gray fields* means species present, but not counted

age	sample	lithology	Chiastozygaceae indet.	Axopodorhabdus cylindratus	Axopodorhabdus sp.	B. constans	C. conicus	C. leptostaurus	C. margerelii	C. tubulata	Cretarhabdus sp.	D. lehmanii	Discorhabdus sp.	E. gallicus	H. cuvillieri	M. permatoidea	P. escaligii	P. madingleyensis	Cretarhabdaceae indet.	S. atmetos	S. bigotii bigotii	S. brevispinus
Middle Volgian	115/1	Black Shale				24,8																
	113/1	Black Shale				13,1					0,6					0,3		0,3	0,6	0,3		
	109/1	Black Shale				15,9				0,3							1,0			0,3		
	103/1	Black Shale				2,2																
	102/1	Claystone																				
	100/1	Calcareous mudstone	0,3			20,7			0,3					0,3				0,3		0,3		
	99/2	Black Shale	2,7			12,3					0,7			0,7				0,7	0,7			
	99/1	Claystone				11,6			1,0		0,7			0,3			0,3					
	95/1	Claystone	1,0			11,7			0,6		1,0									0,6		
	93/1	Claystone				15,5			0,3					0,3								
	92/1	Calcareous mudstone	0,6			6,9			0,3		1,2			0,3			0,3	0,6	0,3			
	91/1	Claystone																				
	90/1	Calcareous mudstone	0,3			1,9								0,3						0,3		
	89/1	Black Shale				12,4			4,8	0,3							0,3					
	88/1	Calcareous mudstone				1,3			1,3	1,3				0,6				0,6				
	86/1	Calcareous mudstone	1,0			10,6	0,3	0,3	1,9	1,0				0,6				0,6		1,3		
	85/1	Claystone				3,1													4,3			
	84/1	Black Shale																				
	82/2	Black Shale	1,0			9,2			4,0					0,7			0,7					
	82/1	Black Shale	3,6			7,2		0,7	0,7		0,3			0,3			0,7		0,3			

sample	lithology	T. intermedius	S.lumina	S. quadriaculla	S. stradneri	W. fossacincta	W. barnesae	W. britannica	W. communis	W. ovata	Watznaueria sp.	Z. fissus	Z. erectus (small)	Z. erectus (big)	Z. erectus (total)	W. barnesae + W. fossacincta	W. britannica + W. communis	individuals encountered	undefined coccoliths	species richness (S)	heterogeneity (H)	equitability (E)	preservation
115/1	Black Shale	1,6		0,3	1,3	7,4	27,7	2,9	15,1	1,9	4,2		6,1	3,9	10,6	35,0	18,0	311	2,9	14	1,93	0,73	E1
113/1	Black Shale					5,5	29,7	5,2	17,7	1,5	5,5		7,3	7,3	14,7	35,2	22,9	327	4,6	14	1,97	0,75	E1-E2
109/1	Black Shale	4,0		0,3	0,7	5,0	38,9	2,7	15,3	1,0	4,3		7,3	1,3	8,6	43,9	17,9	296	1,7	16	1,89	0,68	E1
103/1	Black Shale					10,5	21,3	5,7	19,7	1,9	32,7		0,3	3,5	3,8	31,7	25,4	315	2,2	8	1,71	0,82	E1
102/1	Claystone					5,5	17,7	5,8	7,2		53,3		0,0	1,9	1,9	23,2	13,0	362	8,6	5	1,23	0,77	E3
100/1	Calcareous mudstone			0,3	1,3	11,0	37,3	6,3	14,3	0,7	0,3	1,0	2,0	2,0	4,0	48,3	20,7	300	1,0	15	1,82	0,67	E1
99/2	Black Shale				1,0	6,6	44,5	0,7	13,3	2,3	1,3	1,7	5,3	2,3	7,6	51,2	14,0	301	3,3	14	1,83	0,69	E1-E2
99/1	Claystone			1,3	0,3	5,6	48,0	2,3	19,9	1,3	1,3	1,0	2,3	0,3	2,6	53,6	22,2	302	2,3	14	1,63	0,62	E1-E2
95/1	Claystone					9,7	59,7	1,3	7,8	1,3	2,6	0,6	1,0	1,0	1,9	69,5	9,1	308		14	1,47	0,56	E2
93/1	Claystone	0,3			0,9	9,2	43,0	0,6	15,2	2,8	3,8	0,3	3,8	1,9	5,7	52,2	15,8	316	1,9	15	1,73	0,64	E1
92/1	Calcareous mudstone				0,3	10,1	65,4	1,2	8,6	2,0	0,3	0,6	0,9	0,3	1,2	75,5	9,8	347		14	1,34	0,51	E1-E2
91/1	Claystone					18,5	30,0	0,3	6,4	0,6	42,5			0,3	0,3	48,6	6,7	313	1,3	8	1,28	0,62	E3
90/1	Calcareous mudstone		5,8			7,4	61,9		5,8	2,3	12,9	0,3		0,3	0,3	69,4	5,8	310	0,3	11	1,34	0,56	E2
89/1	Black Shale	0,9			0,3	12,7	53,8	3,6	0,6	0,6	5,1	0,3	3,0	0,6	3,6	66,5	4,2	331	0,6	15	1,58	0,59	E1-E2
88/1	Calcareous mudstone					22,3	50,0	3,8	3,8	3,2	10,5			1,3	1,3	72,3	7,6	314		19	1,56	0,54	E2
86/1	Calcareous mudstone	0,3		0,3		4,5	39,2	13,2	8,4	0,6	10,0	0,3	1,3	2,6	3,9	43,7	21,5	311	1,6	18	2,01	0,71	E1-E2
85/1	Claystone					6,6	38,9	4,3	7,4		33,9			1,6	1,6	45,5	11,7	246		6	1,55	0,86	E3
84/1	Black Shale																	0					
82/2	Black Shale				2,0	3,3	20,5	14,2	22,1	2,0	10,6		1,3	7,3	8,6	23,8	36,3	303	1,3	16	2,15	0,79	E1
82/1	Black Shale				1,3	0,7	21,2	25,4	16,9	3,9	9,8	0,3	3,6	2,6	6,2	21,8	42,3	326	0,7	14	2,12	0,80	E1-E2

a

the marlstones (averaged 27%, maximum 50%) than in the black shales (averaged 8.6%). TOC and $CaCO_3$ are negatively correlated (r=–0.354; Fig. 7a), $\delta^{13}C_{org}$ and TOC shows a positive correlation (r=0.498; Fig. 7b).

Variations in clay mineralogy—observations

For clay mineral analysis, 42 samples of the Kashpir section were studied. Smectite, illite and kaolinite are the predominant clay minerals in all of the examined samples (Fig. 6). Kaolinite decreases in abundances from more than 50% in the lowermost part to 10% at the top of the section. Smectite steadily increases from less than 10% to nearly 50% in the upper part. Illite only slightly increases in abundance from base to top. In contrast to these findings another trend is clearly obvious. Parallel to the positive $\delta^{13}C$ excursions in the black shale layers, smectite also abruptly increases within these intervals at the expense of illite.

Discussion

Calcareous nannofossils

Preservation—theories

In our study, most of the investigated samples yield high relative abundances of *Watznaueria* spp. In the lower part of the Kashpir section, *Watznaueria* spp. makes up more than 74% of the total assemblages both in well-preserved and in poorly preserved samples. In Gorodische, *Watznaueria* spp. shows very high relative abundances (up to 73%) in some of the moderately preserved samples.

sample	lithology	*Axopodorhabdus* sp.	*B. constans*	*C. conicus*	*C. leptostaurus*	*C. margerelii*	*C. salebrosum*	*C. tubulata*	*Cretarhabdus* sp.	*D. lehmanii*	*E. gallicus*	*M. pemmatoidea*	*P. escaigii*	*P. madingleyensis*	Cretarhabdaceae indet.	*S. atmetos*	*S. comptus*	*S. geometricus*	*T. intermedius*	*Tegumentum* sp.	*S quadriaculta*	*S. stradneri*
98/3	Black Shale																					
98/2	Black Shale																					
98/1	Black Shale																					
97/10	Calcareous mudstone																					
97/9	Calcareous mudstone		14,6								0,3				0,3	0,7						
97/8	Calcareous mudstone		42,8										0,3		0,3	0,3			2,3		1,0	
97/7	Calcareous mudstone		52,4				0,3				0,3		0,3		0,6	0,3			3,6		0,6	
97/6	Calcareous mudstone		45,2										0,6			0,6			4,2		1,6	
97/5	Calcareous mudstone		57,5								0,9		0,9		1,3	0,3			4,7		1,3	
97/4	Calcareous mudstone		51,2												0,6				4,0		1,6	
97/3	Calcareous mudstone		45,5	1,0			3,3				0,7		1,0		0,7	0,3			2,0		1,7	
97/2	Calcareous mudstone		51,7				0,6				0,6				0,6	0,9			6,0		2,5	
97/1	Calcareous mudstone		36,3										1,0			1,7	0,3		6,3		1,0	
96/6	Black Shale																					
96/5	Black Shale																					
96/4	Black Shale																					
96/3	Black Shale																					
96/2	Black Shale																					
96/1	Black Shale																					
95/11	Calcareous mudstone		29,9						0,3				0,3		0,6	2,3			0,3	0,3	3,2	1,0
95/10	Calcareous mudstone		32,2						0,3		0,3		1,6		0,9	1,9			0,6		3,4	
95/9	Calcareous mudstone		26,4		0,3				0,7				1,0			0,7					2,0	
95/8	Calcareous mudstone		26,1								0,3		0,6		0,9	0,3			3,5		2,2	
95/7	Calcareous mudstone		28,5	0,3	0,7				0,7		1,0		0,3		0,7	1,3			2,3		3,9	1,0
95/6	Calcareous mudstone		30,9	0,3									1,0		0,3	1,0					2,3	
95/5	Calcareous mudstone		32,7	0,6	0,3				0,3				1,0		1,3	0,3			1,6		1,3	
95/4	Calcareous mudstone		14,3					0,3	0,6				0,3		0,6	0,3			0,3		1,3	
95/3	Calcareous mudstone		19,3		0,3				0,3				0,3		0,6						3,5	0,3
95/2	Calcareous mudstone		4,1						0,3	1					1,6							
95/1	Calcareous mudstone		3,1	0,3					0,6						0,6	0,3					4,6	0,3
94/5	Black Shale		3,6	1,6							0,3		0,6		0,6	0,3					1,0	
94/4	Black Shale																					
94/3	Black Shale																					
94/2	Black Shale																					
94/1	Black Shale																					
93/5	Calcareous mudstone	0,3	10,5										0,3			1,6			6,9		1,6	
93/4	Calcareous mudstone		17,1	0,3					0,3		0,3		0,3			1,3		0,3	7,6		1,0	
93/3	Calcareous mudstone		19,1	0,9							1,2		0,6			0,6			5,7		2,4	
93/2	Calcareous mudstone		12,2						0,3							0,6			4,2		1,6	
93/1	Calcareous mudstone		23,3	0,3		0,3			0,7							0,7			11,5		2,6	
92/1	Black Shale																					
91/5	Calcareous mudstone		6,6						0,6							0,3					0,3	
91/4	Calcareous mudstone		13,7	0,6							0,3		1,0			1,6			3,5		2,5	0,3
91/3	Calcareous mudstone		15,5	0,3		0,3					0,3		1,0			0,6			0,6		1,0	0,3
91/2	Calcareous mudstone		8,8								0,3		0,3			0,3			6,5		3,3	0,7
91/1	Calcareous mudstone		1,7	0,3											0,3							
90/1	Black Shale																					
89/4	Calcareous mudstone																					
89/3	Calcareous mudstone		0,7																			
89/2	Calcareous mudstone		3,0																		0,7	
89/1	Calcareous mudstone		1,8	0,6						0,3					0,6							
88/1	Black Shale																					
87/5	Calcareous mudstone		13,0												0,6	0,6			0,3		1,9	
87/4	Calcareous mudstone		1,6	0,3		0,3									0,6	0,6						
87/3	Calcareous mudstone		7,1			0,9			0,6						0,9						1,2	
87/2	Calcareous mudstone		10,1			0,6		0,3			0,6					0,6			1,3		2,8	
87/1	Calcareous mudstone		20,1	0,3		0,3			0,3					0,3	0,9	0,9			0,3		1,5	

Fig. 5 b

sample	lithology	*W. fossacincta*	*W. barnesae*	*W. britannica*	*W. communis*	*W. ovata*	*Watznaueria* sp.	*Z. erectus* (small)	*Z. erectus* (big)	*Z. erectus* (total)	*W. barnesae + W. fossacincta*	*W. britannica + W. communis*	individuals encountered	undefined coccoliths	species richness (S)	heterogeneity (H)	equitability (E)	preservation
98/3	Black Shale																	
98/2	Black Shale																	
98/1	Black Shale																	
97/10	Calcareous mudstone																	
97/9	Calcareous mudstone	19,3	14,3		8,6	1,0	35,2	0,7	1,3	2,0	33,6	8,6	301	11	11	1,10	0,46	E1
97/8	Calcareous mudstone	7,7	19,6		12,5	1,0	2,6	3,9	1,3	5,1	27,3	12,5	311	14	14	0,89	0,34	E2
97/7	Calcareous mudstone	5,8	15,9	0,3	10,7	0,3	2,3	2,3	1,9	4,2	21,7	11,0	309	5	14	0,79	0,30	E1
97/6	Calcareous mudstone	11,9	16,8		11,0	0,3	2,3	3,2	1,0	4,2	28,7	11,0	310	4	13	0,89	0,35	E1
97/5	Calcareous mudstone	3,1	8,8	0,3	10,1	0,9	2,5	3,1	1,3	4,4	11,9	10,4	318	8	14	0,71	0,27	E1-E2
97/4	Calcareous mudstone	6,2	14,3		10,9	0,6	1,6	3,7	1,6	5,3	20,5	10,9	322	12	15	0,79	0,29	E1
97/3	Calcareous mudstone	5,9	14,9	0,3	11,9	1,0	2,3	5,0	2,6	7,6	20,8	12,2	303		15	0,90	0,33	E1
97/2	Calcareous mudstone	4,1	12,2	0,3	12,2	0,3	2,8	3,1	0,6	3,8	16,3	12,5	319	4	16	0,81	0,29	E1
97/1	Calcareous mudstone	11,3	16,7		13,0	1,0	5,7	3,7	1,0	4,7	28,0	13,0	300	3	16	1,91	0,69	E1, O1
96/6	Black Shale																	
96/5	Black Shale																	
96/4	Black Shale																	
96/3	Black Shale																	
96/2	Black Shale																	
96/1	Black Shale																	
95/11	Calcareous mudstone	15,9	15,9	1,6	11,7	1,0	1,9	5,5	3,9	9,4	31,8	13,3	308	13	16	2,02	0,73	E1
95/10	Calcareous mudstone	12,8	12,2	1,9	13,1	0,3	1,3	8,4	2,5	10,9	25,0	15,0	320	20	15	1,97	0,73	E1
95/9	Calcareous mudstone	11,9	19,8	1,0	16,2	0,7	4,0	9,6	2,3	11,9	31,7	17,2	303	11	13	1,95	0,76	E1-E2
95/8	Calcareous mudstone	11,6	24,5	0,6	14,2	1,3	2,8	5,7	2,5	8,2	36,2	14,8	318	8	13	1,98	0,77	E1
95/7	Calcareous mudstone	19,0	11,1	1,6	7,2	0,3	2,3	10,2	4,3	14,4	30,2	8,9	305	10	15	2,15	0,79	E1
95/6	Calcareous mudstone	16,3	12,6	1,7	12,0	0,7	1,7	6,6	10,3	16,9	28,9	13,6	301	7	13	1,97	0,77	E2
95/5	Calcareous mudstone	13,3	10,4	0,3	9,4	1,0	7,8	5,2	9,1	14,2	23,6	9,7	309	12	14	2,04	0,77	E2
95/4	Calcareous mudstone	19,4	14,0	0,6	17,1	1,6	3,2	12,7	7,3	20,0	33,3	17,8	315	17	15	2,01	0,74	E1
95/3	Calcareous mudstone	14,2	7,6	3,2	23,4	0,3	5,7	11,7	5,7	17,4	21,8	26,6	316	11	15	2,06	0,76	E1
95/2	Calcareous mudstone	29,6	8,0	5,4	24,8	1,3	6,4	7,3	8,6	15,9	37,6	30,3	314	7	12	1,96	0,79	E1, E0
95/1	Calcareous mudstone	25,7	7,1	2,5	12,7	0,3	3,4	22,0	10,8	32,8	32,8	15,2	323	18	15	1,96	0,73	E1, E0
94/5	Black Shale	43,0	13,9	3,9	11,7	2,6	4,2	3,2	8,4	11,7	57,0	15,5	309	3	12	1,89	0,76	E1, E0
94/4	Black Shale																	
94/3	Black Shale																	
94/2	Black Shale																	
94/1	Black Shale																	
93/5	Calcareous mudstone	17,8	20,7	2,0	27,6	1,3	0,7	4,3	3,0	7,2	38,5	29,6	304	4	14	1,97	0,75	E1
93/4	Calcareous mudstone	14,3	24,1	2,2	16,5	0,6	0,0	9,2	2,9	12,1	38,4	18,7	315	3	14	2,05	0,78	E2
93/3	Calcareous mudstone	15,5	18,2	3,9	14,9	1,8	2,7	6,3	4,5	10,7	33,7	18,8	335	3	13	2,22	0,86	E1
93/2	Calcareous mudstone	24,7	19,9	9,0	12,2	1,6	2,2	4,8	3,8	8,7	44,6	21,2	312	5	12	2,07	0,83	E1
93/1	Calcareous mudstone	16,1	16,7	3,0	7,5	2,6		6,2	5,9	12,1	32,8	10,5	305	3	13	2,11	0,82	E1-E2
92/1	Black Shale																	
91/5	Calcareous mudstone	28,0	13,5	6,6	30,5	1,6	6,0	0,3	3,5	3,8	41,5	37,1	318	7	12	1,78	0,72	E1-E2
91/4	Calcareous mudstone	19,1	15,9	4,5	21,3	1,9	1,3	5,1	5,1	10,2	35,0	25,8	314	7	14	2,17	0,82	E1-E2
91/3	Calcareous mudstone	22,6	26,8	2,9	15,8	1,9		3,5	3,5	7,1	49,4	18,7	310	9	15	1,91	0,71	E2
91/2	Calcareous mudstone	20,8	19,9	6,5	19,2	1,6		5,2	2,9	8,1	40,7	25,7	307	11	14	2,06	0,78	E1-E2
91/1	Calcareous mudstone	19,8	12,2	11,9	21,8	0,7	24,4	0,0	6,3	6,3	32,0	33,7	303	2	9	1,82	0,83	E3
90/1	Black Shale																	
89/4	Calcareous mudstone																	
89/3	Calcareous mudstone	36,1	36,7	4,9	5,2	1,3	5,2	1,0	7,5	8,5	72,8	10,2	305	4	8	1,52	0,73	E2
89/2	Calcareous mudstone	28,7	44,6	1,3	10,2	1,7	3,3	1,0	4,3	5,3	73,3	11,6	303	4	10	1,51	0,65	E1
89/1	Calcareous mudstone	33,7	37,6	3,3	14,0	0,6	3,6	0,3	3,3	3,6	71,3	17,3	335	1	11	1,55	0,65	E1
88/1	Black Shale																	
87/5	Calcareous mudstone	30,6	25,6	1,2	13,0	0,3		7,4	2,2	9,6	56,2	14,2	324	11	13	1,74	0,68	E1
87/4	Calcareous mudstone	52,7	21,6	2,2	9,8	1,6	2,2	0,3	5,1	5,4	74,3	12,1	315	3	11	1,47	0,61	E1
87/3	Calcareous mudstone	38,0	36,4	2,5	4,0	0,6	3,4	1,5	0,6	2,2	74,4	6,5	324	7	12	1,56	0,63	E1
87/2	Calcareous mudstone	27,7	37,7	5,0	2,5	1,3	3,8	1,3	1,9	3,1	65,4	7,5	318	8	15	1,78	0,66	E1-E2
87/1	Calcareous mudstone	26,9	29,9	5,3	7,7	1,5		0,6	0,6	1,2	56,8	13,0	338	9	14	1,75	0,66	E1-E2

sample	lithology	*Axopodorhabdus* sp.	*B. constans*	*C. conicus*	*C. leptostaurus*	*C. margerelii*	*C. salebrosum*	*C. tubulata*	*Cretarhabdus* sp.	*D. lehmanii*	*E. gallicus*	*M. pemmatoidea*	*P. escaigii*	*P. madingleyensis*	Cretarhabdaceae indet.	*S. atmetos*	*S. comptus*	*S. geometricus*	*T. intermedius*	*Tegumentum* sp.	*S quadriaculla*	*S. stradneri*
98/3	Black Shale																					
98/2	Black Shale																					
98/1	Black Shale																					
97/10	Calcareous mudstone		14,6								0,3											
97/9	Calcareous mudstone		42,8																			
97/8	Calcareous mudstone		52,4				0,3				0,3											
97/7	Calcareous mudstone		45,2																			
97/6	Calcareous mudstone		57,5								0,9											
97/5	Calcareous mudstone		51,2																			
97/4	Calcareous mudstone		45,5	1,0			3,3				0,7		1,0									
97/3	Calcareous mudstone		51,7				0,6				0,6											
97/2	Calcareous mudstone		36,3										1,0									
97/1	Black Shale																					
96/6	Black Shale																					
96/5	Black Shale																					
96/4	Black Shale																					
96/3	Black Shale																					
96/2	Black Shale																					
96/1	Black Shale																					
95/11	Calcareous mudstone		29,9								0,3		0,3		0,6	2,3			0,3	0,3	3,2	1,0
95/10	Calcareous mudstone		32,2								0,3		1,6		0,9	1,9			0,6		3,4	
95/9	Calcareous mudstone		26,4		0,3						0,7		1,0			0,7					2,0	
95/8	Calcareous mudstone		26,1										0,6		0,9	0,3			3,5		2,2	
95/7	Calcareous mudstone		28,5	0,3	0,7						0,3		0,3		0,7	1,3			2,3		3,9	1,0
95/6	Calcareous mudstone		30,9	0,3							1,0		1,0		0,3	1,0					2,3	
95/5	Calcareous mudstone		32,7	0,6	0,3										1,3	0,3			1,6		1,3	
95/4	Calcareous mudstone		14,3										0,3		0,6	0,3			0,3		1,3	
95/3	Calcareous mudstone		19,3		0,3								0,3		0,6						3,5	0,3
95/2	Calcareous mudstone		4,11			1							0,3									
95/1	Calcareous mudstone		3,11	0,3									0,6		1,6	0,3					4,6	0,3
94/5	Black Shale		3,6	1,6											0,6	0,3			1,6		1,0	
94/4	Black Shale										0,3		0,6									
94/3	Black Shale																					
94/2	Black Shale																					
94/1	Black Shale																					
93/5	Calcareous mudstone	0,3	10,5																			
93/4	Calcareous mudstone		17,1	0,3							0,3		0,3		1,3	0,3			1,6		6,9	
93/3	Calcareous mudstone		19,1	0,9									0,3		0,6	0,3			7,6		1,0	
93/2	Calcareous mudstone		12,2								1,2		0,6		0,6	2,4			5,7		2,4	
93/1	Calcareous mudstone		23,3	0,3							0,3				0,7	1,6			4,2		1,6	
92/1	Black Shale														0,7	2,6			11,5		2,6	
91/5	Calcareous mudstone		6,6								0,6					0,3					0,3	
91/4	Calcareous mudstone		13,7	0,6									1,0		1,6	0,3			3,5		2,5	0,3
91/3	Calcareous mudstone		15,5	0,3							0,3		1,0		0,6	0,3			0,6		1,0	0,3
91/2	Calcareous mudstone		8,8								0,3		0,3			0,3			6,5		3,3	0,7
91/1	Calcareous mudstone		1,7	0,3											0,3							
90/1	Black Shale																					
89/4	Calcareous mudstone																					
89/3	Calcareous mudstone		0,7																			
89/2	Calcareous mudstone		3,0																			0,7
89/1	Black Shale										0,3				0,6							
88/1	Black Shale																					
87/5	Calcareous mudstone		13,0																			
87/4	Calcareous mudstone		1,6	0,3											0,6	0,6			0,3		1,9	
87/3	Calcareous mudstone		7,1				0,3								0,9				1,2			
87/2	Calcareous mudstone		10,1				0,9				0,6				0,6				2,8			
87/1	Calcareous mudstone		20,1	0,3					0,3										1,5			

sample	lithology	*W. fossacincta*	*W. barnesae*	*W. britannica*	*W. communis*	*W. ovata*	*Watznaueria* sp.	*Z. erectus* (small)	*Z. erectus* (big)	*Z. erectus* (total)	*W. barnesae + W. fossacincta*	*W. britannica + W. communis*	individuals encountered	undefined coccoliths	species richness (S)	heterogeneity (H)	equitability (E)	preservation
98/3	Black Shale																	
98/2	Black Shale																	
98/1	Black Shale																	
97/10	Calcareous mudstone																	
97/9	Calcareous mudstone																	
97/8	Calcareous mudstone																	
97/7	Calcareous mudstone																	
97/6	Calcareous mudstone																	
97/5	Calcareous mudstone																	
97/4	Calcareous mudstone																	
97/3	Calcareous mudstone																	
97/2	Calcareous mudstone																	
97/1	Calcareous mudstone																	
96/6	Black Shale																	
96/5	Black Shale																	
96/4	Black Shale																	
96/3	Black Shale																	
96/2	Black Shale																	
96/1	Black Shale																	
95/11	Calcareous mudstone	11,3	16,7		13,0	1,0	5,7	3,7	1,0	4,7	28,0	13,0	300	3	16	1,91	0,69	E1,O1
95/10	Calcareous mudstone	4,1	12,2	0,3	12,2	0,3	2,8	3,1	0,6	3,8	16,3	12,5	319	4	16	0,81	0,29	E1
95/9	Calcareous mudstone	5,9	14,9	0,3	11,9	1,0	2,3	5,0	2,6	7,6	20,8	12,2	303		15	0,90	0,33	E1
95/8	Calcareous mudstone	6,2	14,3		10,9	0,6	1,6	3,7	1,6	5,3	20,5	10,9	322	12	15	0,79	0,29	E1
95/7	Calcareous mudstone	3,1	8,8	0,3	10,1	0,9	2,5	3,1	1,3	4,4	11,9	10,4	318	8	14	0,71	0,27	E1-E2
95/6	Calcareous mudstone	19,3	14,3		8,6	1,0	35,2	0,7	1,3	2,0	33,6	8,6	301	11	11	1,10	0,46	E1
95/5	Calcareous mudstone	7,7	19,6		12,5	1,0	2,6	3,9	1,3	5,1	27,3	12,5	311	14	14	0,89	0,34	E2
95/4	Calcareous mudstone	5,8	15,9	0,3	10,7	0,3	2,3	2,3	1,9	4,2	21,7	11,0	309	5	14	0,79	0,30	E1
95/3	Calcareous mudstone	11,9	16,8		11,0	0,3	2,3	3,2	1,0	4,2	28,7	11,0	310	4	13	0,89	0,35	E1
95/2	Calcareous mudstone	3,1	8,8	0,3	10,1	0,9	2,5	3,1	1,3	4,4	11,9	10,4	318	8	14	0,71	0,27	E1-E2
95/1	Calcareous mudstone	6,2	14,3		10,9	0,6	1,6	3,7	1,6	5,3	20,5	10,9	322	12	15	0,79	0,29	E1
94/5	Black Shale	5,9	14,9	0,3	11,9	1,0	2,3	5,0	2,6	7,6	20,8	12,2	303		15	0,90	0,33	E1
94/4	Black Shale	4,1	12,2	0,3	12,2	0,3	2,8	3,1	0,6	3,8	16,3	12,5	319	4	16	0,81	0,29	E1
94/3	Black Shale	11,3	16,7		13,0	1,0	5,7	3,7	1,0	4,7	28,0	13,0	300	3	16	1,91	0,69	E1,O1
94/2	Black Shale																	
94/1	Black Shale																	
93/5	Calcareous mudstone	14,2	7,6	3,2	23,4	0,3	5,7	11,7	5,7	17,4	21,8	26,6	316	11	15	2,06	0,76	E1
93/4	Calcareous mudstone	29,6	8,0	5,4	24,8	1,3	6,4	7,3	8,6	15,9	37,6	30,3	314	7	12	1,96	0,79	E1,E0
93/3	Calcareous mudstone	25,7	7,1	2,5	12,7	0,3	3,4	22,0	10,8	32,8	32,8	15,2	323	18	15	1,96	0,73	E1,E0
93/2	Calcareous mudstone	24,7	19,9	9,0	12,2	1,6	2,2	4,8	3,8	8,7	44,6	21,2	312	5	12	2,07	0,83	E1
93/1	Calcareous mudstone	16,1	16,7	3,0	7,5	2,6		6,2	5,9	12,1	32,8	10,5	305	3	13	2,11	0,82	E1-E2
92/1	Black Shale																	
91/5	Calcareous mudstone	28,0	13,5	6,6	30,5	1,6	6,0	0,3	3,5	3,8	41,5	37,1	318	7	12	1,78	0,72	E1-E2
91/4	Calcareous mudstone	19,1	15,9	4,5	21,3	1,9	1,3	5,1	5,1	10,2	35,0	25,8	314	7	14	2,17	0,82	E1-E2
91/3	Calcareous mudstone	22,6	28,8	2,9	15,8	1,9		3,5	3,5	7,1	49,4	18,7	310	9	15	1,91	0,71	E2
91/2	Calcareous mudstone	20,8	19,9	6,5	19,2	1,6		5,2	2,9	8,1	40,7	25,7	307	11	14	2,06	0,78	E1-E2
91/1	Calcareous mudstone	19,8	12,2	11,9	21,8	0,7	24,4	0,0	6,3	6,3	32,0	33,7	303	2	9	1,82	0,83	E3
90/1	Black Shale																	
89/4	Calcareous mudstone																	
89/3	Calcareous mudstone	36,1	36,7	4,9	5,2	1,3	5,2	1,0	7,5	8,5	72,8	10,2	305	4	8	1,52	0,73	E2
89/2	Calcareous mudstone	28,7	44,6	1,3	10,2	1,7	3,3	1,0	4,3	5,3	73,3	11,6	303	4	10	1,51	0,65	E1
89/1	Calcareous mudstone	33,7	37,6	3,3	14,0	0,6	3,6	0,3	3,3	3,6	71,3	17,3	335	1	11	1,55	0,65	E1
88/1	Black Shale																	
87/5	Calcareous mudstone	30,6	25,6	1,2	13,0	0,3		7,4	2,2	9,6	56,2	14,2	324	11	13	1,74	0,68	E1
87/4	Calcareous mudstone	52,7	21,6	2,2	9,8	1,6	2,2	0,3	5,1	5,4	74,3	12,1	315	3	11	1,47	0,61	E1
87/3	Calcareous mudstone	38,0	36,4	2,5	4,0	0,6	3,4	1,5	0,6	2,2	74,4	6,5	324	7	12	1,56	0,63	E1
87/2	Calcareous mudstone	27,7	37,7	5,0	2,5	1,3	3,8	1,3	1,9	3,1	65,4	7,5	318	8	15	1,78	0,66	E1-E2
87/1	Calcareous mudstone	26,9	29,9	5,3	7,7	1,5		0,6	0,6	1,2	56,8	13,0	338	9	14	1,75	0,66	E1-E2

Fig. 5 b

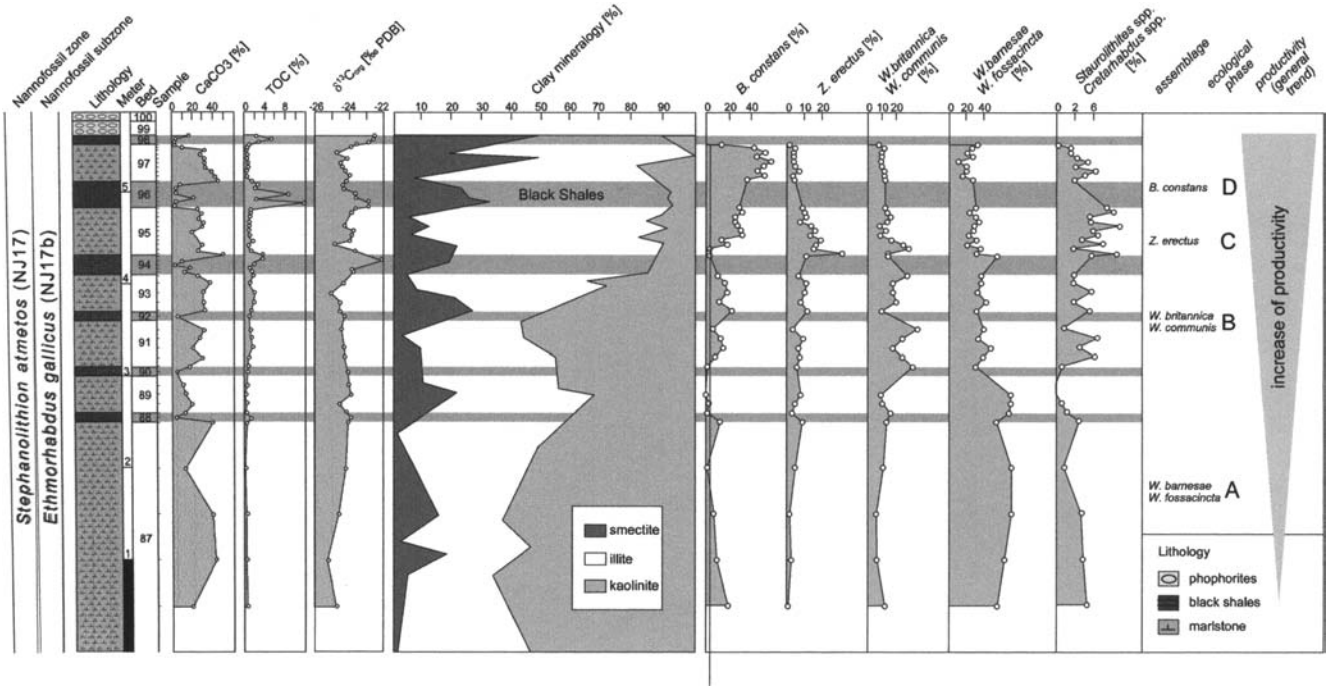

Fig. 6 Lithology, $CaCO_3$, TOC, $\delta^{13}C_{org}$, clay minerals and calcareous nannofossils of the Kashpir section

Due to its size and robustness *Watznaueria* is considered not to be susceptible to dissolution and for this reason resistant to diagenesis. Cretaceous samples containing more than 40% of this genus are thought to be heavily affected by diagenesis (Roth and Bowdler 1981; Roth and Krumbach 1986). On the other hand *Watznaueria barnesae* (the most abundant taxon of this genus) is also interpreted to be a eurytopic species (Mutterlose 1991) and only assemblages including more than 70% of this taxon indicate diagenetic alteration (Williams and Bralower 1995). Some authors suggest that high percentages of *W. barnesae* may also reflect extreme paleoecological conditions (Erba 1992; Erba et al. 1992; Thomsen 1989; Young and Bown 1991; Watkins 1989). Otherwise nannofossils of late Jurassic age are in general more homogeneous and of lower diversity, containing higher abundances of *Watznaueria* spp. than assemblages of Cretaceous age.

The uniform stratigraphic occurrence of small and delicate dissolution-susceptible species like *B. constans*, *S. atmetros* and especially *T. intermedius* in nearly all of the coccolith bearing samples indicates a pristine nannofloral signal. For this reason a significant alteration of the samples can be ruled out and the high abundances of *Watznaueria* are here thought to be controlled by primary factors. Causes for the lack of calcareous nannofossils in the black shale beds of the Kashpir section are discussed later.

Paleoecology—theories

The paleoecological interpretation of calcareous nannofossils in our study is based on the following observations:

- In recent oceans highly diverse assemblages are indicative of stable conditions, in particular oligotrophic warm surface waters (e.g., McIntyre 1967; McIntyre et al. 1970; Brand 1994), reflecting a K-selected evolution.
- Low diversity assemblages are considered to be typical for unstable conditions and cool surface waters enriched with nutrients (e.g., Okada and Honjo 1973; Brand 1994); r-selection is typical for this setting.
- In the fossil record, *W. barnesae* is considered to be an ecologically robust form that is one of the first species to settle in new biotopes (Mutterlose 1991).
- A dominance of *B. constans* and *Zeugrhabdotus* spp. (20–30%) is considered to be indicative for higher productivity of the surface water (Roth 1986; Roth and Bowdler 1981; Roth and Krumbach 1986; Watkins 1989; Erba 1987, 1989; Erba et al. 1992). Therefore, an assemblage rich in *B. constans* and *Zeugrhabdotus* spp. is typical for continental margins with intense upwelling of cold water rich in nutrients (e. g., Roth and Bowdler 1981) or shallow epicontinental seas characterized by intensified storm mixing and high continental nutrient runoff.
- Erba (1992), Williams and Bralower (1995) and Fisher (1999) have observed different responses (different maximum abundances) to changes in surface water fertility for *B. constans* and *Zeugrhabdotus* spp.
- Pittet and Mattioli (2002) have observed a trophic preference continuum represented by successive maximum abundances of different taxa.
- *Crucibiscutum salebrosum*, which is more common in the high latitudes, is viewed as a cool water species which inhibits low latitudinal sites only during specific

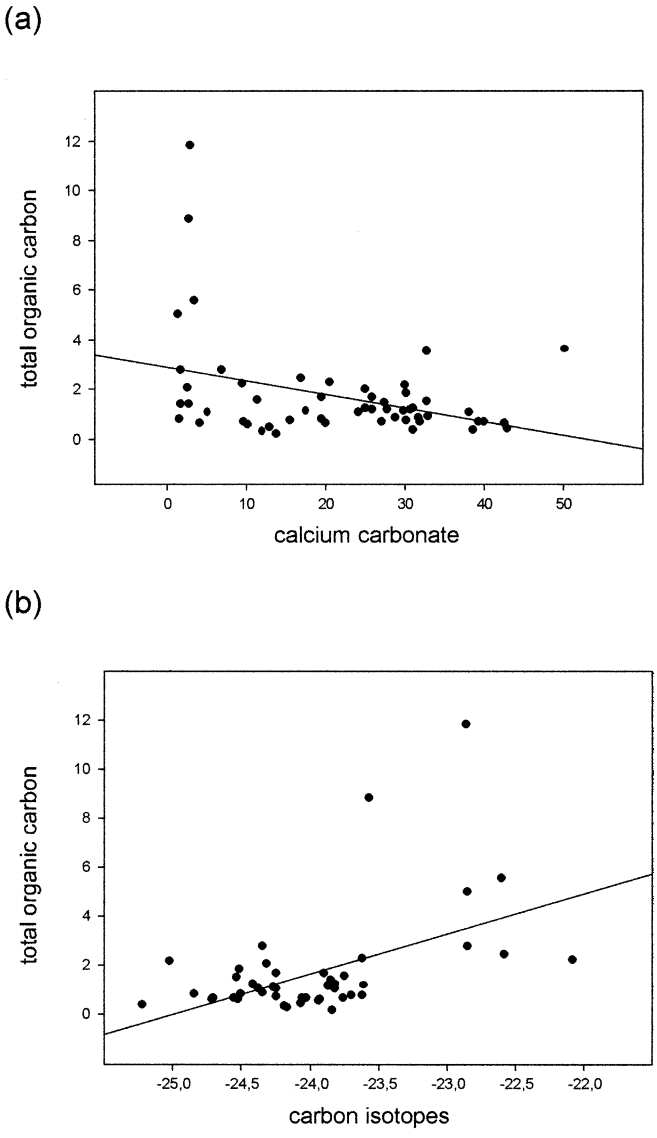

Fig. 7 Scatter plots and linear regressions of the Kashpir section: **a** TOC (%) vs. $CaCO_3$ (%), and **b** TOC (%) vs. $\delta^{13}C_{org}$.(‰ V-PDB)

intervals (e.g., Kessels et al., in preparation; Melinte and Mutterlose 2001; Mutterlose and Kessels 2000; Street and Bown 2000).

- Mutterlose (1996) suggested for *Cretarhabdus* spp. an affinity to more oligotrophic, warm water conditions.
- The ecological affinity of the genus *Staurolithites* spp. is still under discussion. According to Williams and Bralower (1995), this group is positively correlated to *B. constans* and therefore indicative for higher productive environments. Eshet and Almogi-Labin (1996) consider *Staurolithites* spp. to have favored strong oligotrophic surface water. Based on its sparse occurrence in all samples *Staurolithites* spp. is here thought to represent more oligotrophic conditions.

Table 1 Nannofossil acmes of the Kashpir section

Nannofossil acme	Beds	Ecological phase
B. constans	95–97	C
Z. erectus	94–95	C
W. britannica–W. Communis	91–94	B
W. barnesae–W. fossacincta	87–89	A

Assemblage composition—interpretation

In the Kashpir section a significant variation of calcareous nannofossil abundances was clearly observed. The most common coccoliths in nearly all of the investigated samples are assigned to the genus *Watznaueria.* This genus makes up more than 75% of the total abundance in the lower part of the Kashpir section. *B. constans* and *Zeugrhabdotus* spp. are the second most common group with highest abundances up to 60%, replacing *Watznaueria* spp. in the upper part of the section. This indicates a change of the floral assemblages from a *Watznaueria* spp. dominated assemblage in the lower part to a *Watznaueria* spp.–*B. constans–Zeugrhabdotus* spp. dominated assemblage in the upper part of this section. In detail, successive maximum abundances of nannofossils can be recognized allowing the differentiation of four different nannofossil acmes. These may indicate an increase of nutrient availability, thus reflecting part of a mesotrophication cycle (Table 1; Fig. 6).

Keeping in mind that *B. constans* and *Zeugrhabdotus* spp. indicate higher fertility conditions of the surface water, whereas *Watznaueria* is more common in settings of lower fertility, the observed nannofossil distribution seems to reflect an increasing mesotrophication of parts of the Volga Basin studied within the *Dorsoplanites pamderi*-zone. The lowermost phase A is characterized by higher abundances of the cosmopolitan, eurytopic *W. barnesae–W. fossacincta* group, indicating stable and oligotrophic conditions. In phase B (with the first occurrence of the black shales) this group is partly replaced by the *W.britannica–W. communis* group, indicating an early mesotrophication of the basin (see also Pittet and Mattioli 2002). This distribution goes along with similar observations by Keupp and Mutterlose (1994), who recognized higher abundances of *W. britannica* slightly predating the early Aptian Fischschiefer (OAE 1a) in NW Germany. In phases C and D, abundances of the opportunistic species *Z. erectus* and *B. constans* increases, mark enhanced mesotrophic conditions of the basin. For these two taxa, Erba (1992), Williams and Bralower (1995) and Fisher (1999) observed various responses to surface water fertility marking different stages of mesotrophication. In the Kashpir section, *Z. erectus* is most abundant in phase C and partly replaced by *B. constans* in the uppermost phase D. This indicates a further increase of the mesotrophic conditions in the Volga Basin. For phase D, extreme low values for heterogeneity and equitability were calculated. This is typical for unstable and meso–eutrophic conditions

reflecting r-selection. In general, species of more oligotrophic affinity (e.g., *Cretarhabdus* spp., *Staurolithites* spp.) are expected to be rather rare in these settings. In both sections their relative abundances vary from 2 to 5%.

Similar nannofossil distribution patterns were also observed by Bischoff and Mutterlose (1998). These authors recognized four periods of consecutive nannofossil acmes during the deposition of organic rich sediments of the Barremian/Aptian boundary interval of NW Germany. Recapitulatory calcareous nannofossils of the Kashpir section are here interpreted to characterize a transition from a low-productive, oligotrophic environment with high abundances of cosmopolitan species (*Watznaueria* spp.) and predominating marlstone sedimentation, to a higher productivity, mesotrophic environment of cooler water temperatures marked by mass occurrences of opportunistic species (*B. constans*, *Z. erectus*) and the deposition of black shales and phosphates.

Clay minerals

Clay minerals—theories

The clay mineral composition of a rock may contain important information about weathering processes on surrounding landmasses and their distances to the area of sedimentation (e.g., Hallam et al. 1991; Ruffell and Batten 1990; Sellwood and Price 1993, Ruffell et al. 2002b). Kaolinite is most abundant in a warm, humid climate with intense chemical weathering, whereas smectite is generally formed under more semi-arid conditions (e.g., Chamley et al. 1983; Singer 1984). Illite tends to be associated with cold and dry climate (Singer 1984). With the aid of clay minerals it is also possible to get information about the proximity of landmasses from which the clay minerals originated. Sea level changes during the time of deposition led to certain clay mineral assemblages (Hallam et al. 1991). Kaolinite tends to be deposited in near shore neritic settings due to its bigger particle size and tendency to flocculation, whereas the small sized smectite aggregates with excellent swelling capacity and accumulated in offshore pelagic settings. So the kaolinite/smectite ratio may also reflect transgressive and regressive periods during the time of deposition. Using clay minerals for paleoclimatic or geographic interpretation requires an estimation of the diagenetic alteration of the sediments. The primary composition of the clay minerals may be changed to illite by diagenetic transformation of smectite via different stages of mixed layer minerals (e.g., Deconick and Chamley 1983; Nadeau et al. 1985). Because of the tectonic stability of the Russian Platform during most of Mesozoic and Paleozoic times, the investigated sediments of the Volga Basin should not be altered by diagenesis. The clay mineral composition seems to reflect a primary signal.

Clay minerals—interpretation

The clay mineral variation in the Kashpir section reveals two clear trends. The general increase in smectite and decrease in kaolinite during the interval of black shale deposition may be interpreted in one of three ways:

1. The black shale–smectite association is suggested by Kennedy et al. (2002) as reflecting bottom-water and early diagenetic reactions between clays and organic matter. Thus organic productivity may control smectite abundance.
2. Conditions of sea-level rise may force kaolinite deposition to be concentrated further away from the site of deposition as facies belts migrate inland.
3. A gradual change in climatic conditions, from kaolinite-producing semi-humid to smectite-producing semi-arid (both probably seasonal).

All three hypotheses are supported by evidence showing that (1) there is a visual correlation between black shales and smectite abundance, (2) condensed phosphate nodule beds above the black shales demonstrate the presence of a major flooding surface that would follow conditions of sea-level rise, and (3) an influx of the clay mineral palygorskite (forms in arid conditions, see Ruffell et al. 2002a, 2002b) suggests an increase in arid or semi-arid conditions on the surrounding landmasses. A similar trend in clay mineral abundances through the Jurassic/Cretaceous boundary interval was also observed at different localities in western Europe and the North Atlantic area (e.g., Daoudi and Deconinck 1994; Deconinck et al. 1985; Hallam et al. 1991; Wignall and Ruffell 1990). The sedimentary record however suggests regressive conditions for the latest Jurassic of Europe. Baraboshkin (1999) shows evaporite deposits in the Caspian region south of the Volga Basin. This, together with the presence of palygorskite, indicates the influence of aridity in the hinterlands. The upward stratigraphic diminution in kaolinite deposition may be the result of this increasing aridity, coupled with conditions of sea-level rise through the *panderi* zone. Above the *panderi* zone, regressive (evaporite forming in the Caspian area) may have been established. Kaolinite was replaced in the clay mineral fraction by smectite, the presence of which is associated with black shale deposition, especially on the scale of individual black shale beds.

$\delta^{13}C_{org}$, TOC and $CaCO_3$—theories and interpretation

In modern plants (since the Miocene) biological carbon fixation during photosynthesis leads to wide ranges of $\delta^{13}C_{org}$ values: approx. −27‰ PDB for C3 plants and −8 to −16‰ PDB for C4 plants (Groecke 2002). For this reason differences in $\delta^{13}C_{org}$ of Cenozoic marine sediments can be caused by changing ratios of terrestrial and marine organic matter (e.g., Newman et al. 1973; Rühlemann et al. 1996). In older sediments, however,

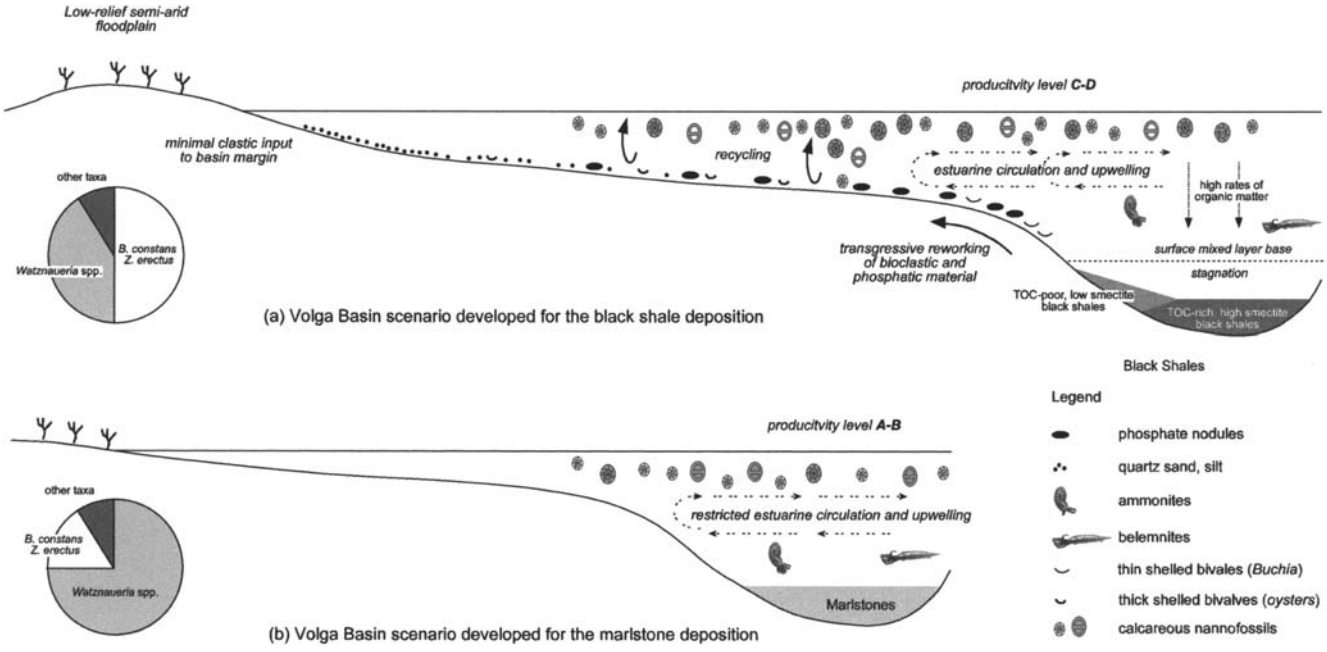

Fig. 8 Proposed depositional model for the Volgian black shales of the Volga Basin

the use of $\delta^{13}C_{org}$ as an indicator of the source of organic matter must be interpreted with caution and only few studies have attained useful results (e.g., Hofmann et al. 2000). Groecke (2002) and Hasegawa et al. (2003) reported on C3 plant organic matter of Cretaceous age with typical values of $\delta^{13}C_{plant}$ −22 to−24‰ PDB which are similar to those of marine derived organic matter.

In the Kashpir section significant positive excursions of $\delta^{13}C_{org}$ (from −24 up to −22‰ PDB) have been observed in nearly all of the black shale horizons. These perturbations of the carbon cycle need some more explanation. Such $\delta^{13}C_{org}$ increases (and the occurrence of black shales), which are well correlated with increases in smectite, may suggest sea-level rises during times of black shale deposition. Sea level rises would finally lead to a declining influx of terrestrial material into the basin, thus positive $\delta^{13}C_{org}$ excursions can possibly be related to changing ratios of terrestrial and marine organic matter.

Due to diagenetic reactions of clay minerals and organic matter, increases of smectite in black shale beds can also be associated with phases of higher primary productivity (Kennedy et al. 2002). Accordingly, Van Kaam-Peters et al. (1998) pointed out that during enhanced primary productivity higher degrees of sulfurization (and therefore increasingly preservation) of isotopically heavy carbohydrates lead to positive rises in $\delta^{13}C_{org}$ This changed the mixing of two isotopic end members ($\delta^{13}C_{lipids}$ and $\delta^{13}C_{carbohydrates}$) and thus explains such $\delta^{13}C_{org}$ fluctuations. Increasing sulfurization can therefore also be related to a positive correlation between TOC and $\delta^{13}C_{org}$, which is clearly documented in the Kashpir section (Fig. 7a). According to Riboulleau et al. (2000), the amorphous organic matter of the kerogen in black shale samples from Gorodische and the lack of lignin-derived pyrolytic products indicate a phytoplanktonic origin of kerogen. Flash pyrolytic analyses also exhibit large contributions of sulfurized carbohydrates in the kerogen. These results seem to support a $\delta^{13}C_{org}$ mixing model to explain the positive $\delta^{13}C_{org}$ excursions in the Kashpir section.

We believe that increases in $\delta^{13}C_{org}$ in the black shale layers of the Kashpir section may be related to enhanced sulfate reduction. This took place during phases of high primary productivity of the surface water, which resulted in higher amounts of carbohydrate carbon. Chemical reactions between organic matter and clay minerals lead to increases in smectite. This assumption would finally also explain the absence of calcareous nannofossils from the black shale beds in the Kashpir section. According to Curtis (1980) and Gardner et al. (1983), increased sulfurization lead to an increase in subsurface acidity in the sediments. This may have resulted in the total dissolution of all coccoliths and may also explain the abrupt decrease in calcium carbonate content resulting in a negative correlation between CaCO3 and TOC (Fig. 7b). These observations are consistent with the poor preservation of calcareous foraminifera in most of these layers (Kuleva et al. 1996).

The depositional environment of the black shales

Using all data available, the following model for the deposition of the Volgian black shales is suggested (Fig. 8). Under a semi-arid climate a change of sedimentation from calcareous mudrocks to black shales occurred. The composition of calcareous nannofossil assemblages, calculated heterogeneity and equitability as well as the

incorporation of geochemical data, suggest that the occurrence of black shales was clearly related to higher primary productivity and the increased nutrient content of the surface water. The occurrence of *C. salebrosum* in the uppermost part of the Kashpir section also indicates that increasing aridity was associated with climatic cooling. This general trend is well correlated with the isotopic results gained from well-preserved belemnites of this section (Riboulleau et al. 1998; Ruffell et al. 2002b; Groecke et al. 2003), giving paleotemperatures of 14–16 °C with a cooling trend towards the late Volgian. In later Jurassic times the topography of the Russian Platform was controlled by tectonic activity (Cimmerian orogenesis), causing small scale morphological changes with swells and troughs. During transgressive periods deeper parts of the basin became oxygen depleted, causing the deposition of organic rich sediments.

Using this depositional model, the origin of enhanced surface water nutrient content needs to be explained. Generally, higher productivity is considered to be associated with more humid climates leading to increased nutrient transfer into oceanic basins or upwelling of nutrient-rich bottom waters. Due to the climatic conditions on the enclosed landmasses, river input did not seem to be the major controlling factor in explaining the high productivity of the Volga Basin. The Volgian scenario may be therefore related to specific water mass movements, especially upwelling of deeper water within different parts of the basin. The general high latitudinal position of the basin (40–50°N), resulting in low solar radiation and cool climate (confirmed by stable isotopes; Riboulleau et al. 1998; Groecke et al. 2003) may have favored the onset of estuarine circulation and the upwelling of bottom water into the photic zone. This caused higher productivity in the surface water and increased phytoplankton growth. Primary production may also be strengthened by the recycling of nutrients from oxidized phytoplankton back into the uppermost water column, providing optimal growing conditions for opportunistic species such as *B. constans* and *Z. erectus*. This productivity system in combination with sea-level rises may have caused black shale deposition in the Volga Basin in mid-Volgian times.

Conclusions

1. Calcareous nannofossils of the lighter colored calcareous mudrock layers of the Kashpir section reflect a pristine sedimentary signal and can be used for paleoecological interpretation. Geochemical analyses show that the absence of coccoliths in the black shales is not primary controlled and can be explained by dissolution during early diagenetic processes.
2. Changes in abundances of calcareous nannofossils represent different stages of mesotrophication of the late Jurassic Volga Basin. The species *B.* constans, *Z. erectus*, *W. britannica/communis* and *W. barnesae/fossacincta* seem to be associated with varying nutrient contents of the surface water.
3. Calcareous nannofossil, clay mineral and isotope data provide evidence that black shale deposition was coupled to enhanced primary productivity of the surface water under a semi-arid climate with a cooling trend to the top of the *panderi* zone.
4. River input from the surrounding landmasses did not seem to be the source of nutrients. More probably, specific watermass movements caused upwelling of recycled nutrients which were partly originated from oxidized phytoplankton.

Acknowledgements Financial support by the Deutsche Forschungsgemeinschaft (Mu 667/19-1) is gratefully acknowledged. Stable isotopes were kindly measured by Dr. B. Donner (Institut für Geowissenschaften, University of Bremen). Alastair Ruffell was supported by a Royal Society travel grant. We are indebted to Evgenij Baraboshkin, Richard Marcinowski and Gregory Price for their help with fieldwork.

Appendix

List of calcareous nannofossils taxa with author attributions and dates

Axopodorhabdus Wind & Wise in Wise 1977
A. cylindratus Noël 1965
Biscutum Black in Black and Barnes 1959
B. constans (Górka 1957) Black in Black and Barnes 1959
Chiastozygus Gartner 1968
C. leptostaurus Cooper 1987
Cretarhabdus Bramlette & Martini 1964
C. conicus Bramlette & Martini 1964
Crucibiscutum Jakubowsky 1986
C. salebrosum (Black 1971) Jakubowsky 1986
Cyclagelosphaera Noël 1965
C. margerelii Noël 1965
C. tubulata (Grün & Zweili 1980) Cooper 1987
Diazomatolithus Noël 1965
D. lehmanii Noël 1965
Discorhabdus Noël 1965
Discorhabdus sp.
Ethmorhabdus Noël 1965
E. gallicus Noël 1965
Hexapodorhabdus Noël 1965
H. cuvillieri Noël 1965
Manivitella Thierstein 1971
M. pemmatoidea (Deflandre in Manivit 1965) Thierstein 1971
Polypodorhabdus Noël 1965
P. escaigii Noël 1965
P. madingleyensis Black 1971
Staurolithites Caratini 1963
S. stradneri Rood et al. 1971
S. lumina Bown 1998
S. quadriaculla (Noël 1965) Rood et al. 1971
Stephanolithion Deflandre 1939

S. atmetos Cooper 1987
S. bigotii Deflandre 1939
S. brevispinus Wind & Wise in Wise 1988
Stradnerlithus Black 1971
S. comptus Black 1971
S. geometricus (Górka 1957) Bown & Cooper 1989
Tegumentum Thierstein in Roth & Thierstein 1972
Truncatoscaphus
T. intermedius Perch-Nielsen 1986
Watznaueria Reinhardt 1964
W. barnesae (Black 1959) Perch-Nielsen 1968
W. britannica (Stradner 1963) Reinhardt 1964
W. communis (Stradner 1963) Reinhardt 1964
W. fossacincta (Black 1971) Bown in Bown & Cooper 1989
W. ovata Bukry 1969
Zeugrhabdotus Reinhardt 1965
Z. erectus (Deflandre in Deflandre & Fert 1954) Reinhardt 1965
Z. fissus Grün & Zweili 1980

References

Baraboshkin EJ (1999) Berriasian–Valanginian (Early Cretaceous) seaways of the Russian Platform Basin and the problem of Boreal/Tethyan correlation. Geol Carpathica 50(1):5–20.

Bersezio R, Erba E, Gorza M, Riva A (2002) Berriasian–Aptian black shales of the Maiolica formation (Lombardian Basin, Southern Alps, northern Italy): local to global events. Palaeogeogr Palaeoclimatogr Palaeoecol 180:253–275

Bischoff G, Mutterlose J (1998) Calcareous nannofossils of the Barremian/Aptian boundary interval in NW Europe: biostratigraphic and palaeoecologic implications of a high resolution study. Cretaceous Res 19:635–661.

Bown P (1998) Calcareous nannofossil biostratigraphy. Chapman and Hall, Cambridge, 314 pp

Brand LE (1994) Physiological ecology of marine coccolithophores. In: Winter A, Siesser WG (eds) Coccolithophores, Cambridge University Press, Cambridge, pp 39–50

Chamley H, Bebrabant P, Chandillier AM, Foulon J (1983) Clay mineralogy and inorganic geochemical stratigraphy of Blake–Bahama Basin since the Callovian, Site 534, Deep Sea Drilling Project Leg. 76. Initial Reports of the Deep Sea Drilling Project 76, US Government Printing Office, Washington, DC, pp 437–451

Coccioni R, Erba E, and Premoli-Silva I (1992) Barremian–Aptian calcareous plankton biostratigraphy from the Gorgo Cerbara section (Marche, central Italy) and implications for plankton evolution. Cretaceous Res 13:517–537

Cooper MKE (1987) New calcareous nannofossil taxa from the Volgian Stage (Upper Jurassic) lectostratotype site at Gorodishche, U.S.S.R. Neues Jahrb Geol Paläontol Monatsh 10:606–612

Curtis CD (1980) Diagenetic alteration in black shales. J Geol Soc Lond 137:189–194

Daoudi L, Deconinck JF (1994) Contrôles paléogéographique et diagénétique des successions sédimentaires argileuses du Bassin Atlasique au Crétacé (Haut-Atlas Occidental, Maroc.). J Afri Earth Sci 18:123–141

Deconinck JF, Chamley H(1983) Héritage et diagenése des minéraux argileux dans les alternaces marno-calcaires du Crétacé inférieur du domaine subalpin. CR Acad Sci 297:589–594

Deconinck JF, Beaudoin B, Chamley B, Joseph P, Raoult JF (1985) Contôles tectonique, eustatique et climatique de la sédimentation argileuse du domaine subalpin francais au Malm-Crétacé. Rev Géol Dynam Geogr Phys 26:311–320

DoddJR, Stanton RJ (1990) Paleoecology—concepts and applications. Wiley, New York, 502 pp

Erba E (1987) Mid-Cretaceous cyclic pelagic facies from the Umbrian–Marchean Basin: What do calcareous nannofossils suggest? INA Newsl 9:52–53

Erba E (1989) Upper Jurassic to Lower Cretaceous Nannoconus distribution in some sections from northern to central Italy. Mem Sci Geol 41:255–261

Erba E (1992) Middle Cretaceous calcareous nannofossils from the western Pacific (Leg 129): evidence for paleoequatorial crossings. In: Larson RL, Lancelot Y, and 21 other editors (ed) Proceedings of the Ocean Drilling Program, scientific results 129, pp 189–201

Erba E, Castradori D, Guasti G, Ripepe M (1992) Calcareous nannofossils and Milankovitch cycles: the example of the Albian Gault Clay Formation (southern England). Palaeogeogr Palaeoclimatogr Palaeoecol 93:47–69

Eshet Y, Almogi-Labin A (1996) Calcareous nannofossils as palaeoproductivity indicators in Upper Cretaceous organic-rich sequences in Israel. Mar Micropalaeontol 26:37–61

Fisher, C. (1999) Calcareous nannofossils as indicators of mid-Cretaceous paleofertility along an ocean front, U.S. western interior. In: Barrera E, Johnson CC (eds) Evolution of the Cretaceous ocean–climate system. Geol Soc Am, Madison, Wisconsin, Special Paper 332, pp 161–180

Gardner WD, Hinga KR, Marra J.(1983) Observations on the degradation of biogenic material in the deep ocean with implications on accuracy of sediment trap fluxes. J Mar Res 38(1):17–39

Gerasimov PA, Mikhailov NP (1966) Volgian stage and the geostratigraphical scale for the upper series of the Jurassic system. Izvest Akad Nauk SSSR, Seriya Geol 2:118–138

Groecke DR (2002) The carbon isotope composition of ancient CO2 based on higher-plant organic matter. Philos Trans R Soc Lond B A 360:633–658

Groecke D, Price GD, Ruffell A, Mutterlose J (2003) Jurassic–Cretaceous palaeotemperatures compared from the Volga Basin (Russian Platform) and Kilhaua Harbour (New Zealand). Palaeoecol Palaeogeogr Palaeoclimatol (in press)

Hallam A, Grose JA, Ruffell AH (1991) Palaeoclimatic significance of changes in clay mineralogy across the Jurassic–Cretaceous boundary in England and France. Palaeogeogr Palaeoclimatogr Palaeoecol 81:173–187

Hantzpergue P, Baudin F, Mitta V, Olferiev A, Zakharov V (1998a) The Upper Jurassic of the Volga basin: ammonite biostratigraphy and correlations with standard European zonations. C RAcad Sci 326:633–640.

Hantzpergue P, Baudin F, Mitta V, Olferiev A, Zakharov V (1998b) The Upper Jurassic of the Volga basin: ammonite biostratigraphy and occurence of organic-carbon rich facies. Correlations between boreal–sobboreal and submediterranean provinces. In: Crasquin-Soleau S, Barrier E (Eds) Peri-Tethys Memoir 4: epicratonic basins of Peri-Tethyan platforms. Mémoires Du Muséum National DHistorique Naturelle, Paris. pp 9–33

Hasegawa T, Pratt LM, Maeda H, Shigeta Y, Okamoto T, Kase T, Uemura K (2003) Upper Cretaceous stable carbon isotope stratigraphy of terrestrial organic matter from Sakhalin, Russian Far East: a proxy for the isotopic composition of paleoatmospheric CO2. Palaeogeogr Palaeoclimatol Palaeoecol 189:97–115

Hofman P, Ricken W, Schwark L, Leythaeuser D (2000) Carbon–sulfur–iron relationships and $\delta^{13}C$ of organic matter for late Albian sedimentary rocks from the north Atlantic Ocean: paleoceanographic implications. Palaeogeogr Palaeoclimatol Palaeoecol 163:97–113

Kennedy MJ (2002) Mineral surface control of organic carbon in black shale. Nature 295:657–660

Keupp H, Mutterlose J (1994) Calcareous phytoplankton from the Barremian/Aptian boundary interval from NW Germany. Cretaceous Res 15:739–763

Kuleva GV, Yanochskina ZA, Bukina TF (1996) Palaeoecosystem of Dorsoplanites *panderi* phase in the Volga shale-generating basin. Stratigr Geol Correlation 4:238–245

Lees JA (2003) Calcareous nannofossil biogeography illustrates palaeoclimate change in the Late Cretaceous Indian Ocean. Cretaceous Res 23:537–634

McIntyre A (1967) Coccoliths as Paleoclimatic indicators of Pleistocene Glaciation. Science 158(3806):1314–1317

McIntyre A, Allan WH, Roche MB (1970) Modern pacific coccolithophorida: a paleontological thermometer Trans N Y Acad Sci 32(6):720–731

Melinte M, Mutterlose . (2001) A Valanginian (Early Cretaceous),Boreal nannoplankton excursion in sections from Romania. Mar Micropalaeontol 43:1–25

Mesezhnikov MS (eds) (1977) Jurassic/Cretaceous boundary beds in the Middle Volga area. Ministry of Geology of the USSR. VNIGRI, pp 1–33

Mutterlose J (1991) Das Verteilungs- und Migrationsmuster des kalkigen Nannoplanktons in der borealen Unter-Kreide (Valangin-Apt) NW-Deutschlands. Palaeontographica B221:27–152

Mutterlose J (1996) Calcareous nannofossil palaeoceanography of the Early Cretaceous of NW Europe. MittGeol Staatsinst Hamburg 77:291–313

Mutterlose J and Kessels K (2000) Early Cretaceous calcareous nannofossils from high latitudes: implications for palaeobiogeography and palaeoclimate. Palaeogeogr Palaeoclimatol Palaeoecol 160:347–372

Nadeau PH, Wilson MJ, Mchardy WJ, Tait JM (1985) The conversion of smectite to illite during diagenesis: evidence from some illitic clay from bentonites and sandstones Mineral Mag 49:393–400

Nalivkin DV (1973) Geology of the USSR. University of Toronto Press, Toronto 855 pp

Newman JW, Parker PL, Behrens EW (1973) Organic carbon isotope ratios in Quaternary cores from the Gulf of Mexico. Geochim Cosmochim Acta 37:225–238

Okada H, Honjo S (1973) The distribution of oceanic coccolithophorids in the Pacific. Deep Sea Res 20:619–641

Perch-Nielsen K (1985) Mesozoic calcareous nannofossils. In: Bolli HM, Saunders JB, Perch-Nielsen K (eds) Plankton stratigraphy. Cambridge University Press, Cambridge pp 329–426

Pittet B, Mattioli E (2002) The carbonate signal and calcareous nannofossil distribution in an upper Jurassic section (Balingen-Tieringen, Late Oxfordian, southern Germany). Palaeogeogr Palaeoclimatol Palaeoecol 179:71–96

Premoli-Silva I, Erba E, Tornaghi ME (1989) Paleoenvironmental signals and changes in surface fertility in mid Cetaceous $C_{org.}$rich pelagic facies of the Fucoid Marls (central Italy). Géobois Mem Spéc 11:225–236

Riboulleau A, Derenne S, Sarret G, Largeau C, Baudin F, Connan J (2000) Pyrolytic and spectroscopic study of a sulphur rich kerogen from the “Kashpir oil shales" (Upper Jurassic, Russian platform). Organic Geochem 0(2000):1–21

Riboulleau A, Baudin F, Daux V, Hantzpergue P, Renard M, Zakharov V (1998) Évolution de la paléotempérature des eaux de la plate-forme russe au cours du Jurassique supérieur. C Rs Acad Sci 326:239–246

Roth PH (1986) Mesozoic palaeoceanography of the North Atlantic and the Tethys Oceans. In: Summerhayes CP, Shackelton NJ (eds) SEPM Special Publication 32, pp 517–546

Roth PH (1989) Ocean circulation and calcareous nannofossil evolution during the Jurassic and Cretaceous. Palaeogeogr Palaeoclimatol Palaeoecol 74:111–126

Roth PH, Bowdler JL (1981) Middle Cretaceous calcareous nannoplankton biogeography and paleoceanography of the Atlantic ocean. SEPM Special Publication 32, pp 517–546

Roth PH, Krumbach KR (1986) Middle Cretaceous calcareous nannofossil biogeography and preservation in the Atlantic and Indian Oceans: implications for paleoceanography. Mar Micropalaeontol 10:235–266

Ruehlemann C, Frank M, Hale W, Mangini A, Mulitza S, Müller PJ, Wefer G (1996) Late Quaternary productivity changes in the western equatorial Atlantic: evidence from ^{230}Th-normalized carbonate and organic carbon accumulation rates. Mar Geol 135:127–152

Ruffell AH, Batten DJ (1990) The Barremian-Aptian arid phase in northern Europe. Palaeogeogr Palaeoclimatol Palaeoecol 80:197–212

Ruffell A, McKinley JM, Worden RH (2002a) Comparison of clay mineral stratigraphy to other proxy palaeoclimate indicators in the Mesozoic of NW Europe. Philos Trans R Soc Lond A 360:675–693

Ruffell AH, Price GD, MutterloseJ, Kessels K, Baraboshkin E, Grocke DR (2002b) Palaeoclimate indicators (clay minerals, calcareous nannofossils, stable isotopes) compared from two successions in the late Jurassic of the Volga Basin (SE Russia). Geol J 37:1–17

Sasonova, I.G. (1977) Die Ammoniten der Jura/Kreide-Grenzschichten der Russischen Plattform. Trudy VNIGRI 185:127 pp

Sasonov, NT, Sasonova IG (eds) (1967) Palaeogeography of the Russian Platform in the Jurassic and Early Cretaceous. Nedra, 227 pp

Sellwood, BW, Price GD (1993) Sedimentary facies as indicators of Mesozoic palaeoclimate. Philos Trans R Soc Lond B341:225–233

Shmur SI, Emets TP, Bartoshevich OV, Kornilina VE, Ermakova VI (1983) Shale bearing layers of the Volga basin. Lithol Mineral Resour 18:337–345

Singer A (1984) The paleoclimatic interpretation of clay minerals in sediments. A review. Earth Sci Rev 21:251–293.

Street C Bown PR (2000) Palaeobiogeography of Early Cretaceous (Berriasian-Barremian) calcareous nannoplankton. Mar Micropaleontol 39:265–291

Thomsen E (1989) Seasonal variation in boreal Early Cretaceous calcareous nannofossils. Mar Micropalaeontol 15:123–152

Tucker M (1988) Techniques in Sedimentology, Blackwell, London, 394 pp

Van Kaam-Peter HME, Schouten S, Köster J, Sinnighe Damste JS (1998) Controls on the molecular and carbon isotopic composition of organic matter deposited in a Kimmeridgian euxinic shelf sea: evidence for preservation of carbohydrates through sulphurisation. Geochim Cosmochim Acta 62: 3259–3283.

Watkins DK (1989) Nannoplankton productivity fluctuations and rhythmically-bedded pelagic carbonates of the Greenhorn Limestone (Upper Cretaceous). Palaeogeogr Palaeoclimatol Palaeoecol 74:75–86

Wignall PB (1994) Black Shales. Clarendon Press, Oxford, 136 pp

Wignall PB, Ruffell AH (1990) The influence of a sudden climatic-change on marine deposition in the Kimmeridgian of northwest Europe. J Geol Soc Lond 147:365–371

Williams JR, Bralower TJ (1995) Nannofossil assemblages, fine fraction stable isotopes, and the paleoceanography of the Valanginian-Barremian (Early Cretaceous) North Sea Basin. Paleoceanography 10(4):815–839

Young JR, Bown PR (1991) An ontogenetic sequence of coccoliths from the Late Jurassic Kimmeridge Clay of England. Palaeontology 34:843–850